

Your Interlibrary Loan request has been sent by email in a PDF format.

If this PDF arrives with an incorrect OCLC status, please contact lending located below.

Concerning Copyright Restrictions

The copyright law of the United States (Title 17, United States Code) governs the making of photocopies or other reproductions of copyrighted materials. Under certain conditions specified in the law, libraries and archives are authorized to furnish a photocopy or other reproduction. One of these specified conditions is that the photocopy or reproduction is not to be "used for any purpose other than private study, scholarship, or research". If a user makes a request for, or later uses, a photocopy or reproduction for purposes in excess of "fair use", that user may be liable for copyright infringement. This institution reserves the right to refuse to accept a copying order if, in its judgment, fulfillment of the order would involve violation of copyright law.

FSU Faculty and Staff: Please refer to Copyright Resources Research Guide for additional information at <http://guides.lib.fsu.edu/copyright>

Interlibrary Loan Services: We Search the World for You...and Deliver!

Interlibrary Loan Services – FSU Community
Florida State University
R.M. Strozier Library
116 Honors Way
Tallahassee, Florida 32306-2047
Email: lib-borrowing@fsu.edu
Website: <https://www.lib.fsu.edu/find-and-borrow/extended-borrowing>
Phone: 850.644.4466

Non-FSU Institutions:

Email: lib-lending@fsu.edu
Phone: 850.644.4466

Rapid #: -23216738

CROSS REF ID: **1086252**

LENDER: **LS1 (University of Sydney) :: Main Library**

BORROWER: **FDA (Florida State University) :: Main Library**

TYPE: Article CC:CCL

JOURNAL TITLE: Solid state physics

USER JOURNAL TITLE: Solid State Physics

ARTICLE TITLE: The Theory and Application of Axial Ising Models

ARTICLE AUTHOR: Julia Yeomans

VOLUME:

ISSUE:

MONTH:

YEAR: 1988

PAGES: 151-200

ISSN: 0081-1947

OCLC #:

Processed by RapidX: 9/30/2024 8:26:34 PM

This material may be protected by copyright (Copyright Act 1968 (Cth))

COMMONWEALTH OF AUSTRALIA

Copyright Regulations 1969

WARNING

This material has been provided to you pursuant to
Section 49 of the copyright Act 1968 (the Act) for
The purposes of research or study. The contents of
The material may be subject to copyright protection
Under the Act.

Further dealings by you with this material may be a
Copyright infringement. To determine whether such a
Communication would be an infringement, it is
Necessary to have regard to the criteria set out in
Part 3, Division 3 of the Act.

The Theory and Application of Axial Ising Models

JULIA YEOMANS

*Department of Theoretical Physics,
Oxford OX1 3NP, England*

I.	Theory	151
1.	Introduction	151
2.	The ANNNI Model.....	153
3.	Theoretical Techniques.....	159
4.	Related Models	168
5.	The Chiral Clock Model.....	176
II.	Experimental Applications	180
6.	Binary Alloys	180
7.	Polytypism	188
8.	Magnetic Systems	196
9.	Conclusion	199

I. Theory

1. INTRODUCTION

The aim of this article is twofold: first, to survey theoretical work on discrete spin models where competition in the Hamiltonian results in modulated ordering, and second, to discuss the relevance of such models to experimental systems.

Two compounds typical of those that will be considered are cerium antimonide and silicon carbide. Cerium antimonide is an Ising ferromagnet which locks in to a large number of different modulated magnetic phases separated by first-order phase transitions. In silicon carbide, on the other hand, the modulation is structural; the close-packed stacking sequence of the component layers can form long period patterns.

The canonical spin model which shows similar behavior is the axial next-nearest-neighbor Ising, or ANNNI, model. The phase diagram of the ANNNI

model contains series of commensurate and incommensurate modulated phases of arbitrarily long wavelength. These are stabilized by entropic effects which dominate because of competition between short-range interactions.

The first half of the article reviews theoretical work on the ANNNI and related models, and the second half describes relevant experimental work. In Section 2 the ANNNI model is defined and its phase diagram elucidated. Emphasis is placed on the physical reasons for the appearance of the modulated phases. This section aims to give a summary which will provide sufficient background to the experimental applications in Section II for those uninterested in theoretical detail.

Section 3 reviews the details of the theoretical methods which have been developed to treat discrete spin models with modulated ordering. Mean-field theory, checked by low-temperature series expansions, has given the greatest insight into the phase diagram.

In order to discuss the relevance of the ANNNI model to modulated ordering in real systems, it is important to consider the effect of new terms in the Hamiltonian on the phase diagram. Therefore, in Section 4, we review results on further-neighbor interactions, the inclusion of quenched or annealed defects, the application of a magnetic field, and the effects of lattice structure.

The final theoretical Section 5 is devoted to the chiral clock model, in which a different mechanism, chiral interactions, provides the competition which leads to modulated phases. The novel interface properties of this model are discussed.

Section 6 opens the experimental section of the article with a discussion of binary alloys where the structural ordering can form long period patterns for some compositions and temperatures. Beautiful high-resolution electron microscopy experiments on these compounds are described. The similar, but less well documented, properties of polytypes are reviewed in Section 7. Then, in Section 8, we discuss the magnetic properties of the cerium monopnictides and their relation to the ANNNI model. The concluding Section 9 points out directions for future research.

A previous review by Bak¹ gives a more general survey of commensurate and incommensurate phases. Shorter summaries of the behavior of the ANNNI model have been published by Selke² and by Yeomans.³

¹ P. Bak, *Rep. Prog. Phys.* **45**, 587 (1982).

² W. Selke, *NATO ASI Ser., Ser. E* **83**, 23 (1984).

³ J. M. Yeomans, *Physica B + C (Amsterdam)* **127B**, 187 (1984).

2. THE ANNNI MODEL.

Perhaps the simplest model where competing interactions lead to modulated structures is the axial next-nearest-neighbor Ising, or ANNNI, model.⁴ The model illustrates much of the essential physics we shall be interested in, and, in this section, we give a description of its phase diagram with particular emphasis on the features found generically in models with competing interactions.

The ANNNI model is an Ising model with a two-state spin, $S_i = \pm 1$, on each lattice site. Interactions are between nearest neighbors, together with a second-neighbor interaction along one lattice direction which we shall call the axial direction, z . Thus the ANNNI model is defined by the Hamiltonian

$$H = -\frac{1}{2}J_0 \sum_{ijj'} S_{i,j}S_{i,j'} - J_1 \sum_{ij} S_{i,j}S_{i+1,j} - J_2 \sum_{ij} S_{i,j}S_{i+2,j} \quad (2.1)$$

where i labels the layers perpendicular to the axial direction and j and j' are nearest-neighbor spins within a layer.

It is useful to note that the ANNNI Hamiltonian, Eq. (2.1), is unchanged under the transformation

$$S_{i,j} \rightarrow -S_{i,j}, \quad i \text{ odd}; \quad J_1 \rightarrow -J_1 \quad (2.2)$$

Hence the phase boundaries are symmetric about $J_1 = 0$ and the phases for $J_1 < 0$ can be determined if those for $J_1 > 0$ are known by flipping every alternate layer of spins.

To identify the regions of the phase diagram where the competition between J_1 and J_2 becomes important, it is helpful to look at the ground state. Note first that within the layers the ordering is always ferromagnetic and that therefore we need only consider the axial direction. The axial ground-state configurations are shown as a function of J_1 and J_2 in Fig. 1. For $J_2 > 0$ there is no competition and the ordering is ferromagnetic or antiferromagnetic for $J_1 > 0$ and $J_1 < 0$, respectively. For $J_2 < 0$, however, the second-neighbor interaction prefers an antiphase configuration, $\cdots \uparrow \downarrow \uparrow \downarrow \cdots$ or $\langle 2 \rangle$, whereas the first-neighbor interaction prefers a simple ferro- or antiferromagnetic state. The former dominates if $|J_1/J_2| < 2$ and hence there are three ground-state phases for $J_2 < 0$.

The boundaries separating these phases have been termed *multiphase lines*^{5,6} because on each of them the ground state is infinitely degenerate. On $J_1/J_2 = -2$, $J_2 < 0$, between $\langle 2 \rangle$ and the ferromagnetic state, $\langle \infty \rangle$, any phase

⁴ R. J. Elliott, *Phys. Rev.* **124**, 346 (1961).

⁵ M. E. Fisher and W. Selke, *Phys. Rev. Lett.* **44**, 1502 (1980).

⁶ M. E. Fisher and W. Selke, *Philos. Trans. R. Soc. London* **302**, 1 (1981).

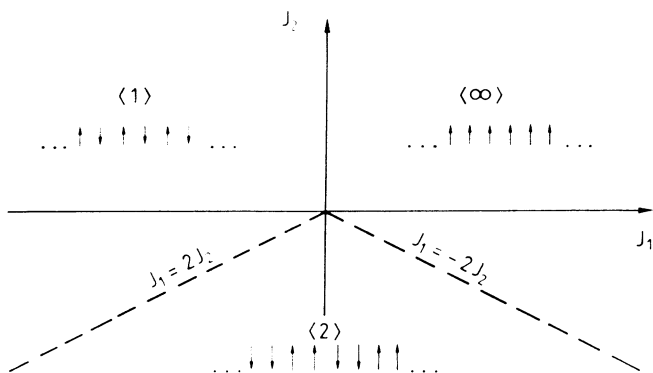


FIG. 1. Ground state of the ANNNI model. —, multiphase boundaries.

containing bands of length two or more has the same energy. Here the term *band* is used to describe a sequence of layers of the same spin value, S , terminated by layers of value $-S$. This is tantamount to saying that any state that can be composed of lengths of the antiphase state, $\langle 2 \rangle$, interspersed with lengths of the ferromagnetic state, is degenerate. Similarly, on the boundary $J_1/J_2 = 2, J_2 < 0$, between the antiferromagnetic ground state, $\langle 1 \rangle$, and $\langle 2 \rangle$, any phase which contains only- and two-bands is degenerate.

In order to describe which of the degenerate ground states remain stable at finite temperatures, it is helpful to introduce a notation which distinguishes between the different axial orderings. We follow Fisher and Selke^{5,6} in taking $\langle n_1, n_2, \dots, n_m \rangle$ to represent a state in which the repeating sequence consists of m bands of length n_1, n_2, \dots, n_m . For example,

$$\cdots \uparrow\uparrow\downarrow\downarrow\uparrow\uparrow\downarrow\downarrow\cdots \quad (2.3)$$

will be denoted $\langle 2223 \rangle$ or $\langle 2^3 3 \rangle$. This ties in with our previous choice of $\langle \infty \rangle$, $\langle 1 \rangle$, and $\langle 2 \rangle$ to describe the ferromagnetic, antiferromagnetic, and antiphase states, respectively.

We now turn to a description of the phase diagram for finite temperatures. The most prominent phases are shown in Fig. 2. The results follow from a mean-field treatment of the ANNNI model on a cubic lattice first carried out by Bak and von Boehm⁷ and later extended by Selke and Duxbury.^{8,9} The modulated phases lie in a region of the phase diagram, bounded by $\langle \infty \rangle$, $\langle 2 \rangle$, and the paramagnetic phase, which springs from the multiphase point and increases in width with increasing temperature. The modulated region is

⁷ P. Bak and J. von Boehm, *Phys. Rev. B*, **21**, 5297 (1980).

⁸ W. Selke and P. M. Duxbury, *Z. Phys. B: Condens. Matter Quanta* **57**, 49 (1984).

⁹ P. M. Duxbury and W. Selke, *J. Phys. A: Math. Gen.* **16**, L741 (1983).

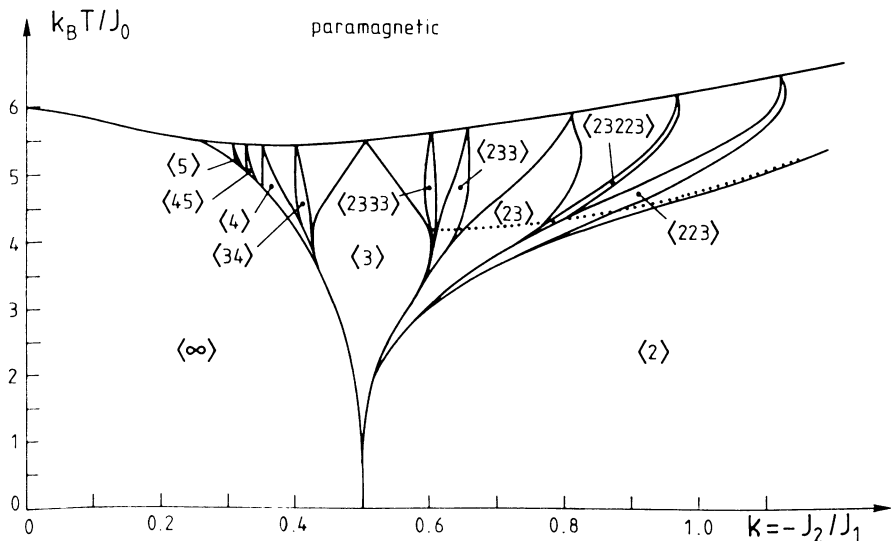


FIG. 2. Mean-field phase diagram of the ANNNI model showing the main commensurate phases,^{7,8} ..., an estimate of the boundary above which incommensurate phases are found between the commensurate phases.¹³

dominated by the shorter period phases, notably $\langle 3 \rangle$. The modulated, paramagnetic, and ferromagnetic phases meet at a Lifshitz point.¹⁰

The phase diagram in Fig. 2 probably best represents what would be seen experimentally: lock in to a few short-wavelength modulated phases separated by first-order phase transitions or by regions where the wave vector appears to vary continuously. However, with better resolution many more commensurate phases would be seen to have a finite field of stability, and it is now believed that infinite sequences of phases appear throughout the phase diagram. These rapidly become very narrow with increasing wavelength, but appear in regular patterns characteristic of models with competing interactions. We shall first consider the stable phases at low temperatures and then describe how new phases become stable as the temperature is raised.

Low-temperature series expansions have enabled the phase sequence in the vicinity of the multiphase point to be calculated.^{5,6,11} Results obtained by Szpilka and Fisher are shown in Fig. 3. An infinite, but very specific sequence of phases, $\langle 2^k 3 \rangle$, springs from the multiphase point. (Throughout this article we shall take k to represent the sequence of non-negative integers, 0, 1, 2, ...) The width of successive phases decreases exponentially with increasing

¹⁰ R. M. Hornreich, M. Luban, and S. Shtrikman, *Phys. Rev. Lett.* **35**, 1678 (1975).

¹¹ A. Szpilka and M. E. Fisher, *Phys. Rev. Lett.* **57**, 1044 (1986).

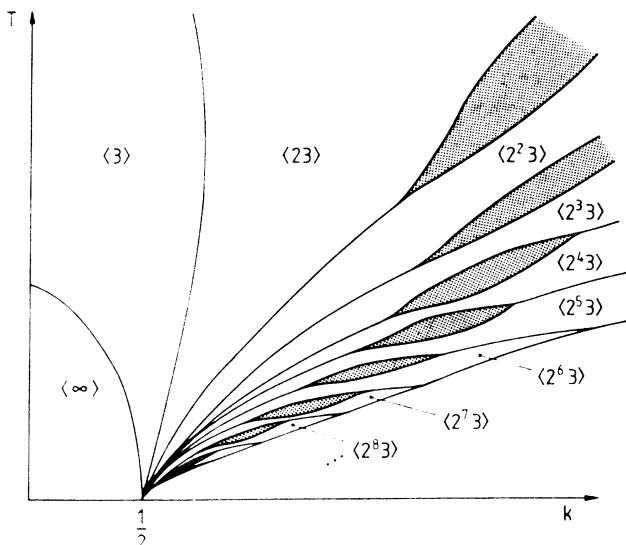


FIG. 3. The ANNNI phase diagram at low temperatures in the vicinity of the multiphase point for $J_1 > 0$.¹¹ Mixed phases, $\langle 2^k 3^{2^{k-1}} 3 \rangle$, are stable in the shaded regions.

k . Phases with successively smaller k cutoff as the temperature is increased, and hence the boundary between $\langle 2 \rangle$ and the modulated region is weakly first order. Mixed phases, $\langle 2^k 3^{2^{k-1}} 3 \rangle$, appear at a temperature which decreases with increasing k , and more complicated combinations may also be stable.¹¹

As the temperature is increased, more phases appear in a systematic way through what has been termed in the literature "structure combination branching processes".^{8,9} In all the cases tested so far, within mean-field theory and low-temperature series, the first new phase to appear between two neighboring phases $\langle a \rangle$ and $\langle b \rangle$ is always $\langle ab \rangle$. Further increases in temperature will cause $\langle a^2 b \rangle$ and $\langle ab^2 \rangle$ to appear on the $\langle a \rangle : \langle ab \rangle$ and $\langle ab \rangle : \langle b \rangle$ boundaries, respectively. Hence sequences of new phases are built up, a typical one of which is shown in Fig. 4.

Selke and Duxbury⁸ checked several series of branching points, and in each case the sequence appeared to extrapolate to an accumulation point below the transition temperature to the paramagnetic phase, T_c . Above the accumulation points one would expect to find commensurate phases with wave vectors corresponding to every rational number within a given interval. As T_c is approached, the widths of the commensurate phases vanish as power laws.^{7,12}

Therefore, above some temperature incommensurate phases must become stable between the commensurate phases.⁷ This behavior is referred to as an

¹² A. Aharony and P. Bak, *Phys. Rev. B* **23**, 4770 (1981).

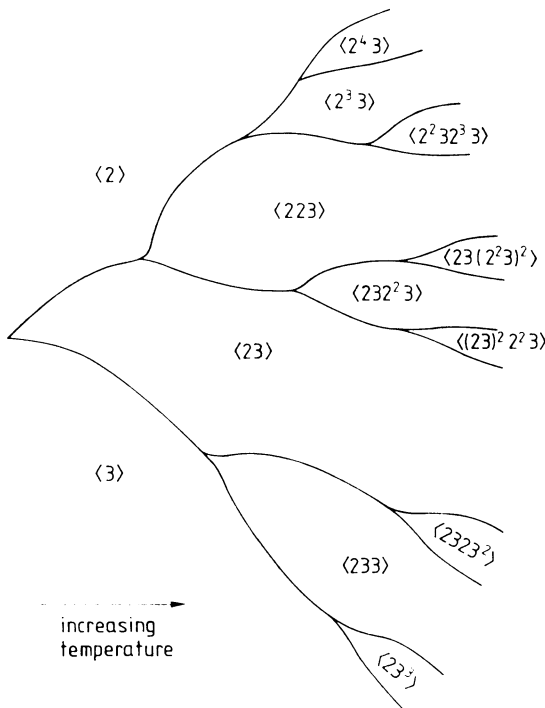


FIG. 4. Schematic representation of a typical structure combination branching sequence.

incomplete Devil's staircase.¹ Some insight into the temperature at which incommensurate phases first appear follows from considering where the energy of interaction between domain walls (where a domain wall can be thought of as a 3-band in the $\langle 2 \rangle$ phase) dominates the energy, pinning the modulated structures to the lattice.^{13,14} The result of a mean-field estimation of this boundary is shown in Fig. 2.

It is important to remember, particularly when using the ANNNI model to represent modulated structures in real systems, that there are an infinite number of metastable states at low temperatures near the multiphase point. Indeed, each stable phase persists as a metastable state when its free energy ceases to provide the global minimum. Free-energy differences between the different metastable states and the stable phase itself can be arbitrarily small. This point, which shows up clearly in mean-field solutions of the model,^{7,9} is of vital importance in the kinetics of modulated structures.

¹³ M. H. Jensen and P. Bak, *Phys. Rev. B* **27**, 6853 (1983).

¹⁴ P. Bak and V. L. Pokrovsky, *Phys. Rev. Lett.* **47**, 958 (1981).

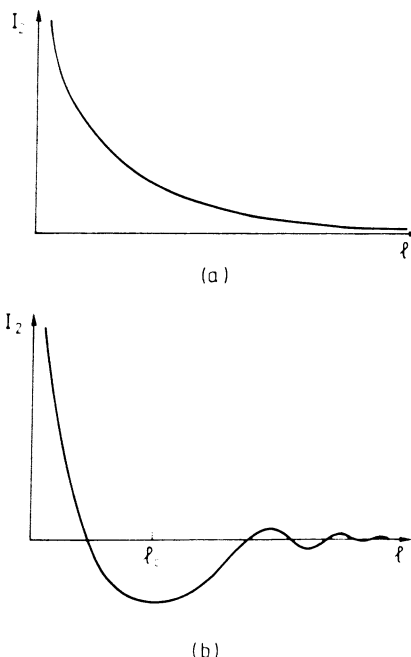


FIG. 5. Possible variation of the interaction, I_2 , between domain walls with distance l .

At this point, leaving details of the theoretical work on the ANNNI phase diagram to the following section, we emphasize some important aspects of the physics which leads to modulated phase sequences. We first stress the importance of entropic contributions to the free energy. Because energy differences are small in the vicinity of the multiphase point, the entropy plays the dominant role in determining the stable phases at finite temperatures.

Entropic effects manifest themselves as fluctuations in the domain walls, where domain walls are most usefully considered to be the structures which destabilize a given commensurate phase (3-bands in the vicinity of $\langle 2 \rangle$; interfaces between up- and down-bands in the vicinity of $\langle \infty \rangle$). As the walls fluctuate they impinge on each other's movement and hence interact.^{11,15}

Consider first only pair interactions between nearest-neighbor walls. Following Szpilka and Fisher,¹⁴ it is useful to distinguish the two cases shown in Fig. 5: (a) the interaction is always repulsive; (b) the interaction has a unique minimum at some spacing, l_c . If only pair interactions are taken into account, the walls are always equidistant at spacing l . In case (a), although it may become favorable, because of a negative wall self-energy, to create walls, they

¹⁵ J. Villain and M. Gordon, *J. Phys. C* **13**, 3117 (1980).

must overcome the repulsive interaction. Hence l decreases monotonically from ∞ , and the transition from the commensurate phase is quasicontinuous. In case (b), however, l_c provides the most favorable spacing, and the transition from the commensurate phase will be first order to a structure with wall spacing l_c .

Case (b) is relevant for the ANNNI model.^{11,15} The transition from $\langle 2 \rangle$ is weakly first order with l_c , the spacing between the three-bands on the boundary, increasing with decreasing temperature to give the onion effect in Fig. 3. Similarly, near $\langle \infty \rangle$, where walls are boundaries between consecutive bands, $l_c = 3$, giving an $\langle \infty \rangle : \langle 3 \rangle$ transition (l_c varies with increasing temperature and decreasing J_0 to give different transitions).

Szpilka and Fisher¹¹ have pointed out that the appearance of mixed phases depends on multiwall interactions. As various combinations of these change sign, new phases appear through structure combination branching processes. It is also of interest to note that the domain wall interactions decay exponentially with distance. This results in the exponential decrease of phase width with increasing period. The calculation of the interaction between domain walls is discussed in Sections 3,b and 3,c.

3. THEORETICAL TECHNIQUES

a. Mean-Field Theory

Mean-field theories have proved to be a very successful tool in the study of models with modulated order.^{4,7,8} Phase diagrams obtained using such approximations appear to be correct in all but minor details. Indeed Szpilka and Fisher¹¹ have studied low-temperature series expansions for general coordination numbers and found that, for the ANNNI model, the mean-field limit agrees with results for lower dimensions. In this section we describe the more conventional theories and then, in Section 3,b, we summarize results due to Villain and Gordon,¹⁵ who have used a mean-field approach to emphasize the role of interactions between domain walls in the formation of the ANNNI phases.

Mean-field theory was first applied to the ANNNI model by Elliott.⁴ He allowed only solutions where the magnetization varied sinusoidally and found that the wave vector varied continuously with $\kappa = |J_2|/J_1$ but was independent of the temperature. Bak and von Boehm^{7,16} were the first to demonstrate the existence of a large number of commensurate phases. Later Duxbury and Selke^{8,9} gave a more detailed picture of certain aspects of the mean-field phase diagram, emphasizing the role of structure combination branching processes.

¹⁶ J. von Boehm and P. Bak, *Phys. Rev. Lett.* **42**, 122 (1979).

The essential difference between the mean-field theory of a model exhibiting modulated order and a simple ferromagnet is that the mean field H_i , must be allowed to vary from layer to layer. The mean-field free energy, F_{mf} , follows as usual from the Bogoliubov inequality¹⁷

$$F_{\text{mf}} = \min(F_0 + \langle H - H_0 \rangle_0) \quad (3.1)$$

where

$$F_0 = -k_B T \ln \left(\sum_{\{S_{i,j}\}} \exp(-H_0/kT) \right) \quad (3.2)$$

In this equation the sum is over all spin configurations, $\{S_{i,j}\}$, and H_0 is a trial Hamiltonian chosen to be

$$H_0 = -\sum_{i,j} H_i S_{i,j} \quad (3.3)$$

Hence the mean field, H_i , appears as a variational parameter associated with the layer i .

Minimizing Eq. (3.1) with respect to the H_i leads to mean-field equations for the average magnetization per layer

$$M_j = \tanh \beta [4J_0 M_j + J_1(M_{j-1} + M_{j+1}) + J_2(M_{j-2} + M_{j+2})] \quad (3.4)$$

where $\beta = 1/k_B T$, and for the free energy

$$\begin{aligned} N^{-2} F_{\text{mf}} = & -NkT \ln 2 + \frac{1}{2}kT \sum_j [(1 + M_j) \ln(1 + M_j) \\ & + (1 - M_j) \ln(1 - M_j)] - \frac{1}{2} \sum_j [4J_0 M_j^2 + J_1 M_j (M_{j-1} + M_{j+1}) \\ & + J_2 M_j (M_{j-2} + M_{j+2})] \end{aligned} \quad (3.5)$$

where there are N^3 spins in the system.

The tanh in Eq. (3.4) may be linearized for small M_i to obtain the transition line between the paramagnetic and ordered phases.⁴ One obtains

$$k_B T_c(\kappa) = 4J_0 + (2 - 2\kappa)J_0, \quad \kappa \leq \frac{1}{4} \quad (3.6)$$

$$= 4J_0 + (2\kappa + 1/4\kappa)J_0, \quad \kappa \geq \frac{1}{4} \quad (3.7)$$

for the boundary to the ferromagnetic and modulated phases, respectively. Near the boundary, for $\kappa > \frac{1}{4}$, the modulated phase is well approximated by a sinusoidal variation of the magnetization with critical wave vector

$$q_c = \cos^{-1}(1/4\kappa) \quad (3.8)$$

Inclusion of umklapp terms indicates that the commensurate phases still

¹⁷ H. Falk, *Am. J. Phys.* **38**, 858 (1970).

exist in this region with widths that vanish as power laws as $T \rightarrow T_c$.⁷ This conclusion has been confirmed using the renormalization group.¹²

At lower temperatures Eq. (3.4) admits, in general, a large number of solutions.⁷⁻⁹ That with the lowest free energy corresponds to the thermodynamically stable phase, with other minima corresponding to metastable states. To find the free energy of a structure of length L the mean-field equations are iterated on a lattice of length L (or $2L$ if there is an odd number of bands) with periodic boundary conditions. The initial conditions are typically taken to be the zero-temperature value of the magnetization in the phase under consideration, and, in general, for stable or strongly metastable states, the fixed point achieved has the same periodicity but a reduced magnetization per layer which depends on the imposed temperature.

The free energy of the trial structure is then calculated and the process repeated for as many structures as necessary. In theory, an infinite trial set is required to be sure of finding the stable phase. This is obviously impossible, and two main approaches have been used in the literature.

In the original calculations⁷ all structures with period up to $L = 17$ were considered. This allowed a study of the overall features of the phase diagram and pinpointed the dominant phases that would be observed in an experiment.

A second approach has been to assume, on the basis of the available numerical evidence and low-temperature series results,⁶ that new phases only appear through structure combination branching processes.^{6,9} This allows a more systematic study of the fine detail in chosen regions of the phase diagram. Selke and Duxbury^{8,9} have used these ideas to show that sequences of branching temperatures converge on an accumulation point.

An interesting approach to the mean-field equations of the ANNNI model is to rewrite them as an iterated map.^{13,18} It is possible to approximate the equations using a two-dimensional mapping¹⁸ or to study the full four-dimensional space

$$M_{i+2} = f(M_{i+1}, M_i, M_{i-1}, M_{i-2}) \quad (3.9)$$

directly.¹³ Limit cycles of the map correspond to commensurate ANNNI phases, and one-dimensional smooth invariant trajectories are identified as incommensurate phases. The physically stable states of minimum free energy correspond to unstable orbits of the map, rendering the numerical work difficult. Chaotic trajectories, which describe metastable states with randomly pinned domain walls, have also been observed.

By searching for the appearance of one-dimensional invariant trajectories with increasing temperature, Jensen and Bak¹³ were able to approximate the line in the phase diagram above which incommensurate phases start

¹⁸ P. Bak, *Phys. Rev. Lett.* **46**, 791 (1981).

appearing. Their estimate is shown by a dotted line in Fig. 2. They argue that incommensurate phases can appear when the interaction between walls dominates the energy pinning them to a particular position on the lattice.^{13,14} These quantities can be calculated numerically within mean-field theory, and equating them gives a boundary for the appearance of incommensurate phases in good agreement with that found from the iterated map.

b. Interactions between Domain Walls

Villain and Gordon¹⁵ studied the ANNNI model using an approach which pinpoints particularly clearly the physical reasons for the existence of the modulated phases. At low temperatures, within a mean-field approximation, they were able to map the model onto a one-dimensional array of interacting domain walls. They showed that the interactions between the walls are long range and oscillatory [type (b) in Fig. 5] and used this to predict the behavior near the multiphase point. In particular, as outlined in Section 2, this approach gives a clear picture of the reason for the initial instabilities of the $\langle \infty \rangle$ and $\langle 2 \rangle$ phase boundaries.

Very recently Szpilka and Fisher¹¹ have shown that, with minor corrections arising from the effect of three-wall interactions, low-temperature series expansions give the same results. They point out that correction terms render the mean-field approach correct only in the intermediate temperature, anisotropic region $q_{\perp} J_0 \gg k_B T \gg \kappa q_{\perp} J_1$, where q_{\perp} and q_1 are the coordination numbers for bonds in and between the layers, respectively. However, the more general low-temperature series analysis confirms that the results remain true as $T \rightarrow 0$.

The mean-field approximation is obtained as before by considering interactions between the average magnetization (per spin) in each layer, m_i .¹⁵ This is allowed to depart from its zero-temperature value, $\sigma_i = \pm 1$, by u_i , giving a Hamiltonian

$$H = -J_1 \sum_i (\sigma_i - u_i)(\sigma_{i+1} - u_{i+1}) \\ - J_2 \sum_i (\sigma_i - u_i)(\sigma_{i+2} - u_{i+2}) + A \sum_i u_i^2 \quad (3.10)$$

where the last term ensures that the u_i remain small. Equation (3.10) may be Fourier transformed to give, after some algebra, a trivial harmonic term together with an effective free energy

$$\tilde{F} = - \sum_{i \neq j} A^2 f(j-i) \sigma_i \sigma_j \quad (3.11)$$

where

$$f(j) = \frac{-1}{8\pi J_2} \int_{-\pi}^{\pi} \frac{dk e^{ikj}}{P(\cos k)} \quad (3.12)$$

with

$$P(x) = x^2 + \frac{1}{2}(J_1/J_2)x - \frac{1}{2} - A/4J_2 \quad (3.13)$$

playing the role of a long-range oscillatory interaction between Ising spins.

To render the physics of the problem transparent, Eq. (3.11) can be rewritten in a form where the variables in the free energy are the position, x_p , of the p th domain wall, where we consider first the situation near $\langle \infty \rangle$ where a domain wall is the boundary between consecutive bands. The resulting free energy¹⁵

$$\tilde{F} = \tilde{F}_0 + n\omega_1 - \sum_{r=1}^x \sum_p (-1)^r U(x_{p+r} - x_p) \quad (3.14)$$

contains three terms. The first is the free energy of the ferromagnetic state. The second is the contribution from n walls each of free energy

$$\omega_1 = 4A^2 \sum_{m=1}^x m f(m) \quad (3.15)$$

and the third with

$$U(j) = -8A^2 \sum_{m=1}^x m f(j+m) \quad (3.16)$$

describes the interaction between r th-neighbor walls.

The mechanism driving the instability of the ferromagnetic phase can be understood by considering just first-neighbor wall-wall interactions. In this case

$$\begin{aligned} U(1) &= -8J_2 > 0 \\ U(2) &= -16(J_1 + J_2)J_2/A > 0 \\ U(3) &= -8J_2^2/A < 0 \\ U(m) &\sim 0, \quad m > 3 \end{aligned} \quad (3.17)$$

at low temperatures. Therefore, we have case (b) of Fig. 5 with $l_c = 3$, and $\langle \infty \rangle$ destabilizes directly to $\langle 3 \rangle$ through a first-order transition.

It is interesting to compare this argument with a similar analysis of the $\langle 2 \rangle$ phase boundary. The destabilizing walls are now three-bands, and Villain and Gordon¹⁵ show that Eq. (3.11) can be rewritten in a way analogous to Eq. (3.14) in terms of the free energy of such defects, together with the interaction between them. The nearest-neighbor interaction is positive for wall separations

$$l \lesssim \frac{\pi}{2} \frac{A^{1/2}}{|J_2|} \quad (3.18)$$

and becomes negative for larger l and then oscillates. Hence the $\langle 2 \rangle$ phase

transforms through a first-order transition to a state with a value of l , l_c , corresponding to the deepest minimum of the interaction potential which is found to be¹⁵

$$2l_c + 1 \approx 2\pi \left[\frac{2}{3} \left(1 - \frac{1}{2} J_1 / |J_2| \right) \right]^{-1/2} \quad (3.19)$$

Note that l_c increases as the multiphase point is approached, giving the sequential cutoff of the phase sequence $\langle 2^k 3 \rangle$ at the $\langle 2 \rangle$ boundary.

In addition to determining the first instabilities of the $\langle \infty \rangle$ and $\langle 2 \rangle$ phases, it is possible to use Eq. (3.14) to establish the infinite phase sequence near the multiphase point. The analysis is similar in spirit to the Fisher-Selke⁶ low-temperature expansion with J_i/A playing the role of the expansion parameters. This calculation is not explicitly laid out in the literature, but similar models have been analyzed in this way.^{19,20}

To conclude, we emphasize that, within a low-temperature mean-field theory, the ANNNI model can be rewritten in terms of a one-dimensional array of interacting domain walls. This point of view will be useful when we consider physical applications of the model in Section II.

c. Low-Temperature Series

A second theoretical method that has been important in establishing the phase diagram of the ANNNI model is low-temperature series expansions. These have been carried out near the multiphase point by Fisher and Selke.^{5,6} The difficulty in applying series techniques to this problem is that, because phases of all lengths are stable, all orders of the expansion are important. For example, the phases $\langle 2^k 3 \rangle$ and $\langle 2^{k-1} 3 \rangle$ are only distinguished by graphs of $k+1$ spin flips. However, Fisher and Selke^{5,6} showed that, by picking out the important terms at each order of the series expansion, it is possible to build up the sequence of phases inductively.

Because of the degeneracy at the multiphase point, it is necessary to expand about all possible ground states. These are distinguished by a set of first-order structural variables, l_k , the number of times per spin a band of length k appears in a given state. For example, for the structure $\langle 2^3 3 \rangle$, $l_2 = \frac{3}{8}$, $l_3 = \frac{1}{8}$, and $l_k = 0$, $k \neq 2, 3$. The structural variables must be non-negative and are related through the constraint

$$\sum_k k l_k = 1 \quad (3.20)$$

E_0 , the ground-state energy per spin, can be written in terms of the structural

¹⁹ J. M. Yeomans, *J. Phys. C* **17**, 3601 (1984).

²⁰ M. Siegert and H. U. Everts, *Z. Phys. B: Condens. Matter Quanta* **60**, 265 (1985).

variables

$$E_0\{l_k\} = -\frac{1}{2}q_{\perp}J_0 - \frac{1}{2}J_1 - J_1\delta\left(2l_2 + l_3 - \sum_{k \geq 5}(k-4)l_k\right) \quad (3.21)$$

where $\delta = \kappa - \frac{1}{2}$.

The low-temperature series expansion for the reduced free energy about a given ground state is, as usual,²¹

$$f\{l_k\} = \frac{-\beta F\{l_k\}}{N} = -\beta E_0\{l_k\} + \sum_{m=1}^x \frac{\Delta Z_N}{N}(m, \{l_k\}) \quad (3.22)$$

where N is the number of lattice sites and $\Delta Z_N(m, \{l_k\})$ is the contribution to the free energy from configurations obtained from the ground state by flipping m spins which, by the linked cluster theorem, will be linear in N .

Defining the Boltzmann factors

$$\begin{aligned} w &= \exp(-2K_0), & x &= \exp(-2K_1), & x^{-1/2-\delta} &= \exp(-2K_2), \\ K_i &= \beta J_i, & i &= 0, 1, 2 \end{aligned} \quad (3.23)$$

and using Eq. (3.20) to eliminate l_3 , the reduced free energy is given to first order by

$$\begin{aligned} f\{l_k\} &= \frac{1}{2}q_{\perp}K_0 + \frac{1}{2}K_1 + K_1\delta/3 + \frac{1}{3}(2 + x^{3+2\delta})w^{q_{\perp}} \\ &\quad + a_2(\delta)l_2 + \sum a_k(\delta)kl_k, \quad k \geq 4 \end{aligned} \quad (3.24)$$

where the structural coefficients

$$a_2(\delta) = 4K_1\delta/3 - \frac{2}{3}(2 - 3x^{1+2\delta} + x^{3+2\delta})w^{q_{\perp}} + O(w^{2q_{\perp}-2}) \quad (3.25)$$

$$\begin{aligned} ka_k(\delta) &= -4K_1\delta(k-3)/3 - [2(k-3)/3 - (k-4)x^{1-2\delta} \\ &\quad - 2x^2 + kx^{3+2\delta}/3]w^{q_{\perp}} + O(w^{2q_{\perp}-2}), \quad k > 3 \end{aligned} \quad (3.26)$$

The stable phases are found by maximizing f with respect to the l_k . As there is a region in which both a_2 and a_k , $k > 3$, are negative, the free energy is maximized by taking the corresponding structural variables to be zero. Hence, from Eq. (3.20), $l_3 = \frac{1}{3}$ and the $\langle 3 \rangle$ phase is stable over a region $O(w^{q_{\perp}})$ between $\langle 2 \rangle$ and $\langle \infty \rangle$.

Fisher and Selke^{5,6} studied the $\langle 3 \rangle : \langle \infty \rangle$ boundary in greater detail by taking the series to third order. They were able to ascertain its shape and, by showing that the surface tension on the boundary is positive, to confirm that the transition is first order. Note, however, that the situation on the $\langle 2 \rangle : \langle 3 \rangle$ boundary is completely different. Here, from Eq. (3.24), it is apparent that all

²¹ C. Domb, *Adv. Phys.* **9**, 149 (1960).

phases which contain only two- and three-bands remain degenerate. Hence it is necessary to proceed to higher orders in the series expansion to ascertain their stability.

To proceed further, one defines a set of higher-order structural variables, l_v , which denote the number of times per layer a band sequence v appears in a given structure. For example, for $\langle 2^3 3 \rangle$, $l_{23} = \frac{1}{9}$, $l_{22} = \frac{2}{9}$, and so on. The higher-order structural variables are not independent but are related through equations like

$$l_{2v3} + l_{2v2} = l_{2v} \quad (3.27)$$

However, Fisher and Selke^{5,6} showed that it is possible to choose an independent subset of the variables and that the free-energy expansion can be written as a linear function of these standard structural variables.

To write down the free-energy expansion to second order, two standard structural variables are needed, l_2 and l_{23} . The second-order contribution to the reduced free energy is then given by

$$f^{(2)} = \Sigma(a_0^{(2)} + a_2^{(2)}l_2 + a_{23}^{(2)}l_{23}) \quad (3.28)$$

where $a_0^{(2)}$, $a_2^{(2)}$, and $a_{23}^{(2)}$, the structural coefficients evaluated to second order, depend on the Boltzmann factors x , δ , and w . The important structural coefficient for our purpose is

$$a_{23}(\delta) = 3(1 - x^2)(1 - x^{1+2\delta})^2 w^{2q_+} + O(w^{3q_+-2}) \quad (3.29)$$

$a_{23}(\delta)$ is positive on the boundary between $\langle 2 \rangle$ and $\langle 3 \rangle$ for $x < 1$. Hence the reduced free energy will be maximized by taking l_{23} to be as large as possible and the $\langle 23 \rangle$ phase will be stable within a region $O(w^{2q_+})$ of this boundary. To proceed further, the new boundaries, $\langle 2 \rangle:\langle 23 \rangle$ and $\langle 23 \rangle:\langle 3 \rangle$, which remain infinitely degenerate, must be examined at higher orders of the series expansion.

Let us now sketch the general order calculation. Consider the k th order of the series expansion, where the phase $\langle 2^{k-1} 3 \rangle$ has just appeared as a stable phase between $\langle 2^{k-2} 3 \rangle$ and $\langle 2 \rangle$. Fisher and Selke^{5,6} were able to show that the first possible instability of the new boundaries $\langle 2^{k-1} 3 \rangle:\langle 2^{k-2} 3 \rangle$ and $\langle 2^{k-1} 3 \rangle:\langle 2 \rangle$ are to $\langle 2^{k-1} 3 2^{k-2} 3 \rangle$ and $\langle 2^k 3 \rangle$, respectively. To check whether these phases are, in fact, stable, it is necessary to calculate the coefficient of the corresponding structural variable in the expansion of the free energy. If this is positive, the new phase will appear; if negative, the phase boundary will remain stable to all orders of the expansion.

Calculating the coefficients is a matter of identifying the important graphs in the expansion of the free energy. The relevant graphs correspond to those one would intuitively expect: linear connected (that is, first- or second-neighbor) chains of spin flips along the axial direction, together with the

corresponding disconnected configurations. A moment's thought shows that these are the lowest-order graphs which can distinguish between different axial orderings. The phase $\langle 2^k 3 \rangle$ is stabilized at order $k + 1$ because this is the number of connected spins that must flip to span the sequence.

Because the important structural coefficients correspond to linear graphs, they are most easily calculated using a transfer matrix method,^{11,22} in which bonds are added one at a time, together with their Boltzmann factors and those of the corresponding disconnected configurations. For the ANNNI model one finds to leading order

$$a_{2^{k-1}32^k+23} = -x^{1+2\delta}(1-x^{1+2\delta})^{2k-2}w^{(2k-3)q}, \quad (3.30)$$

which is negative, and hence the $\langle 2^{k-1}3 \rangle : \langle 2^{k-2}3 \rangle$ boundary is stable. However,

$$a_{2^k3} = (k+2)(1-x^2)(1-x^{1+2\delta})^{k+1}w^{(k+1)q}, \quad (3.31)$$

is positive and, to order $k + 1$, $\langle 2^k 3 \rangle$ appears between $\langle 2^{k-1} 3 \rangle$ and $\langle 2 \rangle$. The analysis must then recommence about the new boundaries. Thus an inductive argument shows that the phase sequence $\langle 2^k 3 \rangle$ springs from the multiphase point of the ANNNI model. The width of the phase $\langle 2^k 3 \rangle$ is $O(w^{(k+1)q_1})$.

It has recently been realized¹¹ that rather subtle correction terms in Eqs. (3.30) and (3.31), which mathematically show up as a degeneracy of the eigenvalues in the transfer matrix used to calculate the coefficients, lead to oscillations for large k . Hence the $\langle 2^k 3 \rangle$ phase sequence is not infinite at any finite temperature and the $\langle 2 \rangle : \langle 2^k 3 \rangle$ boundary is weakly first order, as first pointed out by Villain and Gordon.¹⁵ Moreover, mixed phases, such as $\langle 2^k 3 2^{k+1} 3 \rangle$ and possibly more complicated structural combinations, appear at low temperatures for large enough k . This is illustrated in Fig. 3.

Finally we note that a calculation of the structural coefficients is tantamount to a calculation of pair (a_{2^k3}) and three-wall ($a_{2^k332^{k+1}3}$) interactions, and the arguments given above can be reformulated in terms of such interactions.

d. Other Approaches

(i) *High-Temperature Series.* It is possible to gain some insight into the behavior of the ANNNI model in the vicinity of the paramagnetic-ordered phase boundaries using high-temperature series. Oitmaa²³ has recently analyzed series of 11 terms for the three-dimensional ANNNI model extending

²² J. M. Yeomans and M. E. Fisher, *Physica A (Amsterdam)* **127**, 1 (1984).

²³ J. Oitmaa, *J. Phys. A: Math. Gen.* **18**, 365 (1985).

earlier work by Redner and Stanley.^{24,25} The transition temperature is decreased by about 25° from the mean-field value, and the Lifshitz point occurs at $|J_2/J_1| = 0.270 \pm 0.005$, in close agreement with the mean-field result of $\frac{1}{4}$. Values for the susceptibility exponent, however, do not show the expected crossover from Ising to $X-Y$ -like behavior as κ is increased beyond the Lifshitz point.²³

(ii) *Monte Carlo.* Monte Carlo work on systems with many modulated phases is beset with difficulties. The most evident of these lies in the impossibility of choosing a lattice size and boundary conditions along the axial direction²⁶ which do not effect the periodicity of the modulation. Moreover, at lower temperatures, the kinetics are sluggish and the system is very likely to get stuck in a metastable state.

Early Monte Carlo work went some way in considering the temperature dependence of the wave vector but was able to find no direct evidence of any discontinuous variation.²⁶⁻²⁸ At higher temperatures Monte Carlo approaches^{29,30} have been used to find the transition line to the modulated phase and the position of the Lifshitz point, giving results in good agreement with the high-temperature series expansions.²³ The values of the critical exponents near the Lifshitz point have also been studied.³⁰

Although it is very difficult to use Monte Carlo algorithms to probe the details of the modulated structures in the ANNNI model, some consideration of the kinetics of phase changes between the different equilibrium phases may prove more fruitful.

4. RELATED MODELS

The main motivation in studying systems which are extensions and modifications of the ANNNI model has been to understand the extent to which the results are applicable to experiment. For example, calculations for the ANNNI model in a magnetic field were undertaken in an attempt to explain neutron scattering results for the cerium monopnictides.³¹ A study of the

²⁴ S. Redner and H. E. Stanley, *J. Phys. C* **10**, 4765 (1977).

²⁵ S. Redner and H. E. Stanley, *Phys. Rev. B* **16**, 4901 (1977).

²⁶ W. Selke and M. E. Fisher, *Phys. Rev. B* **20**, 257 (1979).

²⁷ W. Selke and M. E. Fisher, *J. Magn. Magn. Mater.* **15-18**, 403 (1980).

²⁸ E. B. Rasmussen and S. J. Knak-Jensen, *Phys. Rev. B* **24**, 2744 (1981).

²⁹ W. Selke, *Z. Phys. B: Condens. Matter Quanta* **29**, 133 (1978).

³⁰ K. Kaski and W. Selke, *Phys. Rev. B* **31**, 3128 (1985).

³¹ V. L. Pokrovsky and G. V. Uimin, *J. Phys. C* **15**, L353 (1982).

effect of third-neighbor interactions^{32,33} and defects³⁴ aimed to understand whether the generic properties of the ANNNI phase diagram can be expected to apply to polytypic compounds and binary alloys where these features must be present.

In this section we review results on ANNNI-like models. We will first concentrate on the theoretical results. Applications to real systems will be discussed extensively in the second half of the review.

a. The ANNNI Model in a Magnetic Field

Several authors^{31,35–42} have studied the effect on the phase diagram of adding a field term, $-H\sum_{i,j} S_{i,j}$ to the ANNNI Hamiltonian, Eq. (2.1). Because the field breaks the symmetry under spin reversal, it is necessary to refine the Fisher-Selke notation⁵ to describe the stable phases. Let bands of spin $S = -1$ be identified by a horizontal bar above the number describing the band width. For example, the states $\cdots \bar{\uparrow}\downarrow\bar{\uparrow}\downarrow\cdots$ and $\cdots \bar{\downarrow}\uparrow\bar{\uparrow}\downarrow\cdots$ are described by $\langle\bar{1}\bar{2}\rangle$ and $\langle\bar{1}2\rangle$, respectively.

The ground state of the ANNNI model in a field can be determined by careful inspection³⁵ or by linear programming.³⁶ The result is shown in Fig. 6 for a value of $H > 0$. For $J_1 > 0$, the phases $\langle\bar{2}\bar{2}\rangle$ and $\langle\infty\rangle$ remain the sole ground states as the field is applied. For $J_1 < 0$, however, the situation is more complicated with a new phase, $\langle\bar{1}2\rangle$, being stable even at zero temperature. Results for $H < 0$ follow immediately by reversing the sign of each spin.

Yokoi *et al.*³⁵ were the first to study the effect of a field on the ANNNI model phase diagram. They used mean-field theory and concentrated mainly on the region near the paramagnetic-modulated phase boundary, modeling the ordered state as a sine wave. They established that the transition temperature is depressed quadratically with the applied field and that the wave vector near the transition depends only on κ , not on field or temperature. It is interesting to note that, within this approximation, the boundary between the modulated and paramagnetic phases changes from second to first order as the field increases. Yokoi *et al.*³⁵ did not systematically study the lock-in to

³² W. Selke, M. N. Barreto, and J. M. Yeomans, *J. Phys. C* **18**, L393 (1985).

³³ M. N. Barreto and J. M. Yeomans, *Physica A (Amsterdam)* **134**, 84 (1985).

³⁴ H. Roeder and J. M. Yeomans, *J. Phys. C* **18**, L163 (1985).

³⁵ C. S. O. Yokoi, M. D. Coutinho-Filho, and S. R. Salinas, *Phys. Rev. B* **24**, 4047 (1981).

³⁶ V. L. Pokrovsky and G. V. Uimin, *Sov. Phys.—JETP (Engl. Transl.)* **82**, 1640 (1982).

³⁷ H. C. Ottinger, *J. Phys. A: Math. Gen.* **16**, 1483 (1983).

³⁸ J. Smith and J. M. Yeomans, *J. Phys. C* **15**, L1053 (1982).

³⁹ J. Smith and J. M. Yeomans, *J. Phys. C* **16**, 5305 (1983).

⁴⁰ G. V. Uimin, *J. Stat. Phys.* **34**, 1 (1984).

⁴¹ A. M. Szpilka, *J. Phys. C* **18**, 569 (1985).

⁴² G. V. Uimin, *Piz'ma — JETP* **36**, 201 (1982).

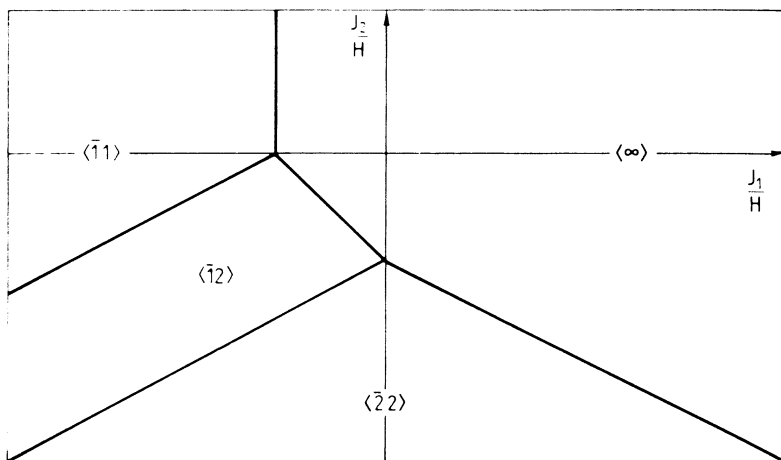


FIG. 6. Ground state of the ANNNI model in a magnetic field for $H > 0$.

commensurate phases at lower temperatures. However, they determined that a large number of commensurate phases do exist and pointed out that those surviving to finite field are, in general, those with a finite magnetization. The mean-field theory of the ANNNI model in a field has also been studied by Ottinger.³⁷

A more thorough study of the low-temperature region of the phase diagram using a low-temperature series expansion analogous to that applied to the zero-field problem by Fisher and Selke^{5,6} has been undertaken by several authors.³⁸⁻⁴¹ Pokrovsky and Uimin^{36,42} have also addressed the problem of the phase diagram at low temperatures using a different expansion technique. They assumed the dominance of the coupling in the layers, $J_1, J_2 \ll J_0$, and then performed a cumulant expansion in the interlayer Hamiltonian.

The behavior near each of the multiphase lines is complicated.³⁸⁻⁴² For those readers interested in the details, we describe the behavior near each line below, but it is first useful to give a summary of the main results and to point out some unusual features of the phase diagram. In general the ANNNI model in a magnetic field behaves in a qualitatively similar manner to the zero-field case. In particular, there are several sequences of modulated phases near the multiphase lines which are generated by the usual structure combination branching processes. As one might have guessed, those of the zero-field phase sequences with a finite magnetization persist as the field is increased, giving phase sequences like $\langle(\bar{2}2)^k(\bar{2}3)\rangle$ and $\langle\bar{1}2(\bar{2}2)^k\rangle$. Uimin⁴⁰ argues that, as the in-plane interactions become less dominant, the harmless Devil's staircases¹ are replaced by complete staircases with all commensurate phases appearing. It is

interesting to note that unusual phases made up from $\bar{1}2$ and $\bar{1}3$ units appear between $\langle \infty \rangle$ and $\langle \bar{1}2 \rangle$.

In more detail, results for specific phase boundaries are as follows:

$$J_1 > 0$$

(i) $\langle \infty \rangle : \langle \bar{2}2 \rangle$ Boundary. As a positive magnetic field is switched on, the multiphase sequence existing in zero field, $\langle 2^k 3 \rangle$, crosses over to $\langle (\bar{2}2)^k \bar{2}3 \rangle$.³⁸⁻⁴² The disappearing phases cut off at a field of order the zero-field phase width.⁴¹ The sequence is replaced by a direct first-order transition between $\langle \infty \rangle$ and $\langle \bar{2}2 \rangle$ for $J_1 \simeq |J_2|$. Uimin has argued that for sufficiently small J_0 the harmless staircase becomes a complete staircase.⁴⁰

$$J_1 < 0$$

(i) $\langle \bar{1}1 \rangle : \langle \bar{1}2 \rangle$ Boundary. There is no splitting on this boundary for sufficiently large J_0 . However, for $|J_2| > J_0$, the phase sequence $\langle (\bar{1}2)^{k+1} \bar{1}1 \rangle$ appears.

(ii) $\langle \bar{2}2 \rangle : \langle \bar{1}2 \rangle$ Boundary. The phase sequence $\langle \bar{1}2(\bar{2}2)^{k+1} \rangle$ is stable. Uimin⁴⁰ argues that this crosses over to a complete staircase as J_0 is decreased.

(iii) $\langle \infty \rangle : \langle \bar{1}2 \rangle$ Boundary. The situation on this boundary is not entirely clear. Structures made up from $(\bar{1}2)$ and $(\bar{1}3)$ band sequences are stable in certain regions of the parameter space.^{36,40}

The main application of these results, to explain the phase diagram of cerium antimonide, is described in Section 8.

b. Further-Neighbor Interactions

It is of interest both academically and in preparation for applying models with competing interactions to experimental systems to consider the effect of the further-neighbor interactions that must inevitably be present in reality. The most obvious extension of the ANNNI model is to an Ising model with both second- and third-neighbor interactions along the axial direction. This has been studied by Selke *et al.*³² using mean-field theory and by Barreto and Yeomans³³ using low-temperature series. The main features of the phase diagram are understood and are qualitatively similar to those described for the ANNNI model. However, there are quantitative differences in the particular sequence of phases stable near a given multiphase line.

The ground state of the axial Ising model with second- and third-neighbor interactions is shown in Fig. 7 for $J_1 > 0$.⁴³ Three of the ground-state phase

⁴³ M. N. Barreto, Ph.D. thesis, Univ. of Oxford, Oxford, England, 1985.

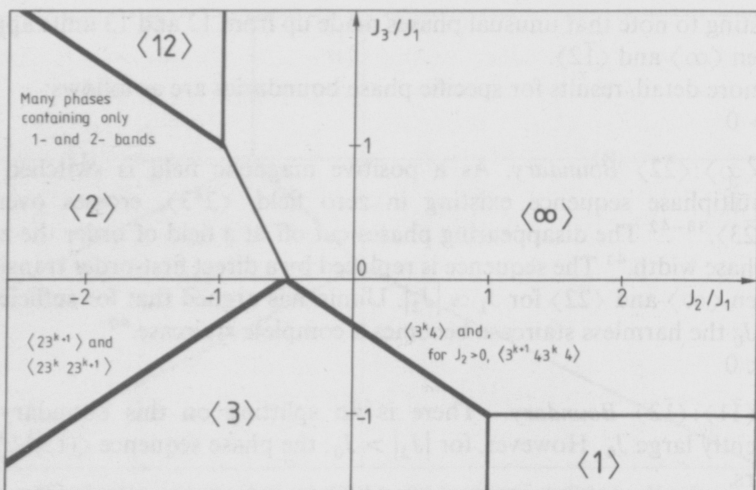


FIG. 7. Ground state of the axial Ising model with third-neighbor interactions for $J_1 > 0$. The phase boundaries shown in bolder type are multiphase lines.

boundaries, shown in bold type in the figure, are multiphase lines close to which one might expect long-wavelength phases to be stabilized. Results for $J_1 < 0$ can be obtained immediately from those for $J_1 > 0$ using the transformation Eq. (2.2) together with $J_3 \rightarrow -J_3$, and therefore we concentrate our attention on the latter case.

We first describe the low-temperature series results,³³ which predict which phases spring immediately from the multiphase point. On the boundary between $\langle \infty \rangle$ and $\langle 3 \rangle$ the phase sequence $\langle 3^k 4 \rangle$ is stable. For $J_2 > 0$ the phases $\langle 3^k 43^{k+1} 4 \rangle$ also appear. Between $\langle 2 \rangle$ and $\langle 3 \rangle$ the sequences $\langle 23^{k+1} \rangle$ and $\langle 23^k 23^{k+1} \rangle$ are stable at the lowest temperatures. On the $\langle 12 \rangle$: $\langle 2 \rangle$ phase boundary many phases containing one- and two-bands, but no neighboring one-bands, spring from the multiphase point: here the situation is too complicated for the phase sequences to be identified using low-temperature series or mean-field theory. These results are summarized in Fig. 7.

Mean-field theory has been used to obtain information about the phase diagram at higher temperatures.³² In all the regions studied new phases were generated as the temperature was raised through the same structure combination branching processes seen in the ANNNI model. An interesting detail is that certain phase sequences cut off with increasing temperature and then reappear. For example, for small $J_3 < 0$, the $\langle 3^k 4 \rangle$ sequence behaves in this way. The points where the phases disappear and reappear coalesce as J_3 becomes more negative.

c. Annealed Vacancies

Again with a view to assessing the relevance of models with competing interactions to real systems, Roeder and Yeomans³⁴ studied the effect of annealed vacancies on the phase diagram of the ANNNI model. Impurities are known to have a significant effect on the stability of long period phases.^{44,45}

Vacancies were introduced through a variable $t_i = 0, 1$ on each lattice site, giving the Hamiltonian

$$H = -\frac{1}{2}J_0 \sum_{ijj'} s_{i,j} t_{i,j} s_{i,j'} t_{i,j'} - J_1 \sum_{ij} s_{i,j} t_{i,j} s_{i+1,j} t_{i+1,j} \\ - J_2 \sum_{ij} s_{i,j} t_{i,j} s_{i+2,j} t_{i+2,j} + D \sum_{ij} t_{i,j} \quad (4.1)$$

The last term is a chemical potential which controls the number of impurities present in the system. Using the transformation $\sigma_{i,j} = s_{i,j} t_{i,j}$, where $\sigma_{i,j}$ is a spin-1 variable, the Hamiltonian in Eq. (4.1) can be rewritten as

$$H = -J_0 \sum_{ijj'} \sigma_{i,j} \sigma_{i,j'} - J_1 \sum_{ij} \sigma_{i,j} \sigma_{i+1,j} \\ - J_2 \sum_{ij} \sigma_{i,j} \sigma_{i+2,j} + D' \sum_{ij} \sigma_{i,j}^2 \quad (4.2)$$

where $D' = D - k_B T \ln 2$.

The phase diagram of this Hamiltonian was investigated using mean-field theory³⁴ for $D' < 0$, where the ground state is the same as that of the ANNNI model, with no layers with $\sigma_{i,j} = 0$. Within mean-field theory the shape of the boundary of the paramagnetic phase is independent of the value of D' , although it moves to lower temperatures as expected as an increasing number of defects inhibit the ordering. Similarly the Lifshitz point remains at the same value of κ but moves to lower temperatures with increasing D' . Moreover, the appearance of the modulated phases is essentially unchanged by the presence of defects.

The defects order in a way that reflects the modulation in the underlying structure, as shown in Fig. 8 for the phase $\langle 23233 \rangle$. The impurities prefer to lie on the boundaries of bands of width greater than two, where they increase the energy of the lattice least. A very good description of the distribution of impurities, especially at lower temperatures, is given by

$$n_i = \exp(E_i/k_B T) \quad (4.3)$$

where E_i is the difference between the energy of a spin and the energy of an

⁴⁴ J. P. Jamet and P. Leaderer, *J. Phys., Lett.* **44**, L257 (1983).

⁴⁵ N. W. Jepps, Ph. D. thesis. Univ. of Cambridge, Cambridge, England, 1979.

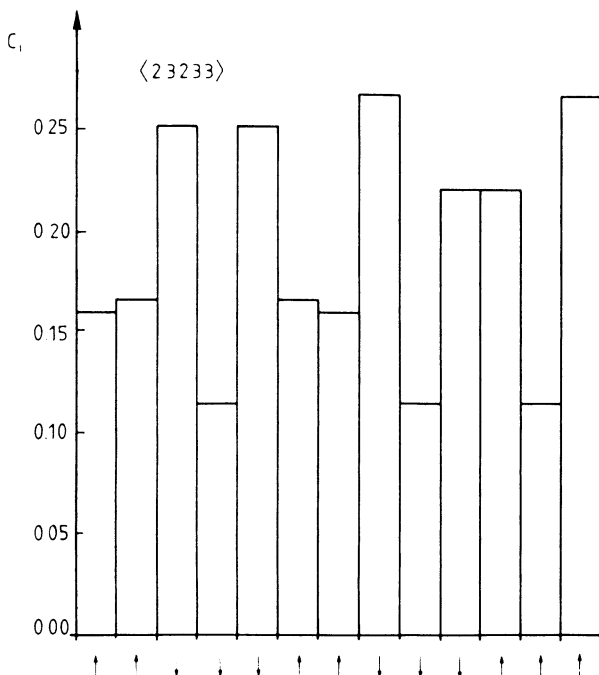


FIG. 8. Distribution of annealed impurities in the $\langle 23233 \rangle$ phase of the ANNNI model. C_i is the percentage impurity concentration in layer i .⁴⁶

impurity in the i th layer. At higher temperatures entropic factors tend to spread the impurities more uniformly throughout the lattice, but this effect causes only a small deviation from a Boltzmann distribution even close to the paramagnetic phase.

By the addition of a term $-K_1 \sum \sigma_{i,j}^2 \sigma_{i+1,j}^2$ it is possible to introduce interactions between the vacancies in the system. However, this again leads to no qualitative change in the phase diagram.⁴⁶ Further work to study the effects of different sorts of impurities on the modulated structures would be of interest.

d. Quenched Impurities

Assessment of the stability of modulated structures in the presence of quenched impurities is a difficult problem, but some attempts have been made in this direction. Fishman and Yeomans⁴⁷ studied the effect of quenched

⁴⁶ H. Roeder, Ph.D. thesis, Univ. of Oxford, Oxford, England, 1986.

⁴⁷ S. Fishman and J. M. Yeomans, *J. Phys. C* **18**, 857 (1985).

random bonds or sites on modulated phases using domain arguments. Defects may locally favor a different phase which will be stabilized if the increase in free energy resulting from the creation of interfaces can be overcome. The domains then round the phase transition, and, if the rounding is greater than the phase width, the phase will be destroyed. Fishman and Yeomans⁴⁷ argue that this is indeed the case for $2 < d < 3$ but that for $d \geq 3$ the modulated phases remain stable against domain formation.

Bak *et al.*⁴⁸ however, look at a different mechanism which can affect the long period ordering in three dimensions. They argue that walls (for example, a band sequence $2^{k-1}3$ in $\langle 2^k 3 \rangle$) can lower their free energy by fluctuating in the presence of the impurities which behave like random fields. In three dimensions such walls become favorable, destroying the parent phase, for periods

$$l > l_c \sim 1/c \quad (4.4)$$

where c is the concentration of defects. Note, however, that the critical length, l_c , may typically be rather large. Nonequilibrium effects are likely to be more important in real systems.

e. Lattice Structure

Nakanishi and Shiba⁴⁹ have considered a model with competing interactions on a lattice which comprises stacked, two-dimensional, triangular layers. Within the layers there are competing first- and second-neighbor interactions, J_1 and J_2 ; along the perpendicular chains the interaction, J_0 , is ferromagnetic. The ground state of this model in a magnetic field is shown in Fig. 9a. Note that structures with two-dimensional modulation are stable.

Nakanishi and Shiba⁴⁹ concentrated on the boundary between the (2×2) and (3×3) ground-state structures. On this boundary it is possible to insert walls separating (3×3) domains with no additional energy. The walls form a triangular structure resulting in phases like that shown in Fig. 9b. As the temperature is increased, mean-field calculations⁴⁹ show that a sequence of such structures with different domain wall spacings are stabilized. This is an interesting attempt to study two-dimensional modulated structures in three dimensions.

In a second paper on the same model, Nakanishi⁵⁰ considers the zero-field case. He discusses the possibility of lines of spins within the triangular layer which have zero average magnetization and their effect on the phase diagram.

⁴⁸ P. Bak, S. Coppersmith, Y. Shapir, S. Fishman, and J. M. Yeomans, *J. Phys. C* **18**, 3911 (1985).

⁴⁹ K. Nakanishi and H. Shiba, *J. Phys. Soc. Jpn.* **51**, 2089 (1981).

⁵⁰ K. Nakanishi, *J. Phys. Soc. Jpn.* **52**, 2449 (1983).

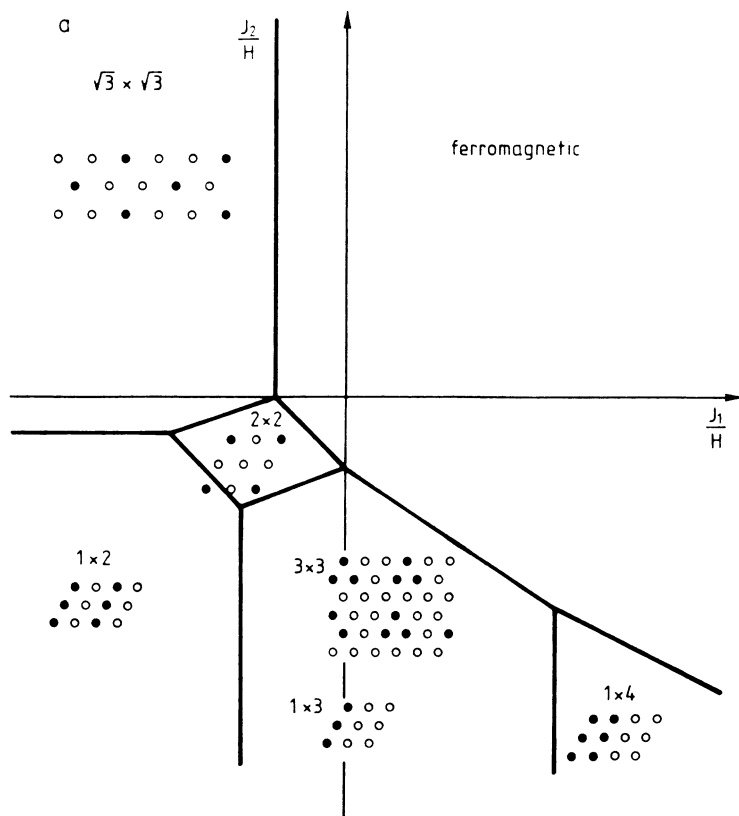


FIG. 9. (a) Ground state of the next-nearest-neighbor Ising model studied by Nakanishi and Shiba.⁴⁹ (b) Phase with a triangular domain wall configuration. Phases of this type with different wall spacings are stable at low temperatures near the multiphase line between the (3×3) and (2×2) phases.

5. THE CHIRAL CLOCK MODEL

A second mechanism through which competition can be introduced into a spin Hamiltonian is by including a term favoring chiral ordering. This is the case in the p -state chiral clock model,^{51,52} which is defined by the Hamiltonian

$$H = -\frac{1}{2}J_0 \sum_{ij} \cos \frac{2\pi}{p} (n_{i,j} - n_{i,j'}) - J \sum_{ij} \cos \frac{2\pi}{p} (n_{i,j} - n_{i+1,j} + \Delta) \quad (5.1)$$

where the $n_{i,j}$ are p -state variables which take values $0, 1, \dots, p-1$. The

⁵¹ S. Ostlund, *Phys. Rev. B* **24**, 398 (1981).

⁵² D. A. Huse, *Phys. Rev. B* **24**, 5180 (1981).

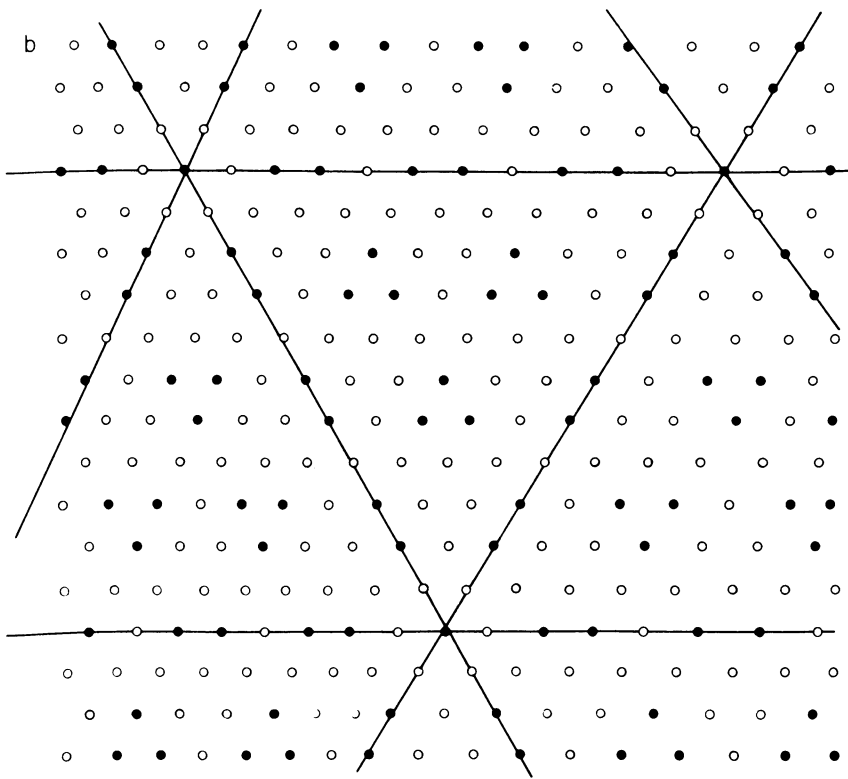


FIG. 9. (Continued)

notation used to distinguish between in-layer and axial bonds follows Eq. (2.1). Note that the partition function is invariant under the transformation and reidentifications

$$\begin{aligned}\Delta &\rightarrow \Delta' = 1 - \Delta \\ n_{i,j} &\rightarrow n_{i,j'} = (-n_{i,j} + i)(\text{mod } p)\end{aligned}\quad (5.2)$$

The phase diagram of the chiral clock model for $p = 3$ is shown in Fig. 10.²² As Δ increases, 01 (and equivalently 12 and 20) bonds become energetically more favorable compared with ferromagnetic bonds, and, at $\Delta = \frac{1}{2}$, the ground state crosses over from ferromagnetic to right-handed chiral ordering ...012012... along the axial direction. $\Delta = \frac{1}{2}$ is a multiphase point, and, as for the ANNNI model, small free-energy differences between the degenerate phases lead to an infinite sequence of commensurate phases springing from this point at finite temperatures.²²

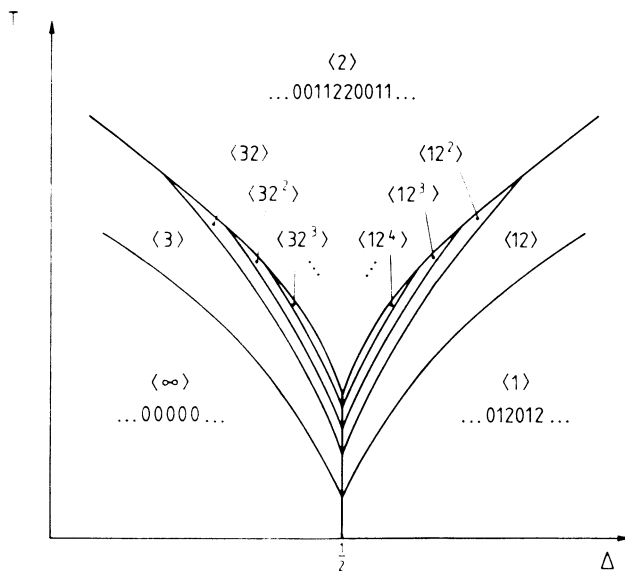


FIG. 10. Low-temperature phase diagram of the three-state chiral clock model.²²

The existence of the phase sequences for a cubic lattice was first established by Yeomans and Fisher^{22,53} using low-temperature series. The stable phases can be described with a notation analogous to that used for the ANNNI model. For example, $\langle 23 \rangle$ represents

$$\dots 00112200112220011122\dots \quad (5.3)$$

For $\Delta = \frac{1}{2}$ the phase $\langle 2 \rangle$ must be stable to satisfy the symmetry properties of the Hamiltonian, Eq. (5.2). Between $\langle 2 \rangle$ and $\langle \infty \rangle$ the stable phase sequence is $\langle 2^k 3 \rangle$, whereas between $\langle 2 \rangle$ and the chiral phase, $\langle 1 \rangle$, one obtains $\langle 12^{k+1} \rangle$. The transition from the $\langle 2 \rangle$ phase is weakly first order, indicating a wall interaction that behaves as shown in Fig. 5b. (Whereas for the ANNNI model the cutoffs of the phase sequence near the $\langle 2 \rangle$ boundary are tricky to establish using low-temperature series,¹¹ the effect follows immediately for the chiral clock model from an obvious change in the sign of the structural coefficients.²²)

Yeomans⁵⁴ has reported the low-temperature series expansion for the chiral clock model for higher values of p . It is difficult to obtain an analytic expression for the structural coefficients as p increases, but they can be

⁵³ J. M. Yeomans and M. E. Fisher, *J. Phys. C* **14**, L835 (1981).

⁵⁴ J. M. Yeomans, *J. Phys. C* **15**, 7305 (1982).

calculated numerically. The series show that the number of stable phase sequences springing from the multiphase point increases with increasing p , with the intervening sequences following the usual structure combination rule.

The mean-field theory of the chiral clock model has been studied extensively.^{19,20,55-57} In particular, Siegert and Everts²⁰ review and extend previous work. An expansion for small magnetization⁵⁶ shows that for

$$\Delta < \Delta_{mc} = \frac{1}{2\pi} \cos^{-1}\left(\frac{1}{2} - J_0/J\right) \quad (5.4)$$

there is a first-order transition from the paramagnetic to the ordered state, whereas for $\Delta > \Delta_{mc}$ the transition is continuous.

As the temperature is lowered the system locks in to a large number of commensurate phases in a way very reminiscent of the ANNNI model. The structure of the phases has been investigated using Landau theory, which includes umklapp terms,²⁰ finite lattice mean-field calculations,⁵⁷ by viewing the mean-field theory as an iterated mapping,^{20,55} and by a method analogous to the Villain–Gordon theory reviewed in Section 3b.^{19,20}

An interesting point that has arisen from these calculations is that the low-temperature series results in three dimensions do not agree in detail with mean-field results.²⁰ Szpilka and Fisher¹¹ have indeed demonstrated that the low-temperature series results are dependent on coordination numbers: mixed phases appear as these are increased from the value pertinent to the cubic lattice.

Recently Huse *et al.*⁵⁸ have pointed out that the chiral clock model exhibits novel interface properties. Consider imposing an interface perpendicular to the axial direction by fixing the left-hand side of the system in state 0 and the right-hand side in state 2. At $\Delta = 0$ this will result in a 0|2 interface. However, as Δ is increased, the energy of a 0|2 interface increases relative to that of a 0|1 or 1|2 interface until, at $\Delta = \frac{1}{4}$, it becomes energetically favorable for the interface to wet to give a configuration 00 ··· 00|11 ··· 11|22 ··· 22, with at least one layer with spins $n_{i,j} = 1$.

Armitstead *et al.*⁵⁹ recently showed that, at finite temperatures, the wetting takes place through a sequence of first-order layering transitions. The number n of layers with $n_{i,j} = 1$ at the interface increases by one at each of the phase boundaries.

⁵⁵ H. C. Ottinger, *J. Phys. C* **16**, L257 (1983).

⁵⁶ H. C. Ottinger, *J. Phys. C* **16**, L597 (1983).

⁵⁷ H. C. Ottinger, *J. Phys. C* **15**, L1257 (1982).

⁵⁸ D. A. Huse, A. M. Szpilka, and M. E. Fisher, *Physica A (Amsterdam)* **121**, 363 (1983).

⁵⁹ K. Armitstead, J. M. Yeomans, and P. M. Duxbury, *J. Phys. A: Math. Gen.* **19**, 3165 (1986).

These results were obtained from low-temperature series using a method analogous to that described for the ANNNI model in Section 3c. The behavior of the phase sequence as the temperature is raised remains an open question—the phases may cutoff, the first-order boundaries could end in a sequence of critical points, or, if the roughening transition does not intervene, could reach the bulk phase boundary.

The 4-state model has somewhat different features.⁶⁰ A 0|3 interface wets to 00 ··· 00|11 ··· 11|22 ··· 22|33 ··· 33 at $\Delta = 2(\tan^{-1} \frac{1}{2})/\pi$ through a single first-order transition from $n = 0$ to $n = \infty$. A 0|2 interface, however, which wets at $\Delta = 0$, has at least two layering transitions.

Although experimental realizations of the chiral clock model in two dimensions have been provided by absorbed layers of H on Fe(110),⁶¹ no similar correspondence has been established in three dimensions. It would certainly be of great interest to find such a system. Meanwhile the model stands as an example of an alternative mechanism leading to competition which can result in modulated ordering when the Hamiltonian contains only short-range interactions.

II. Experimental Applications

6. BINARY ALLOYS

Gradually evidence has been mounting that the ANNNI model is not just a theorist's playground but that it has considerable experimental relevance. Perhaps this is not so unexpected. It has long been acknowledged that a two-state system can be mapped onto an Ising model, often with just short-range interactions.⁶² If the effective coupling between nearest-neighbor spins turns out to be small, the second-neighbor interaction can be important, and, if it is antiferromagnetic, modulated phases can appear.

Several authors have pointed out that the ANNNI model mirrors many of the features seen in binary alloys.^{63–65} Long period structures are primarily observed in compounds containing noble metals, for example, Ag₃Mg,^{66,67}

⁶⁰ P. J. Upton, Univ. of Oxford, Oxford, England (unpublished work).

⁶¹ I. Sega, W. Selke, and K. Binder, *Surf. Sci.* **154**, 331 (1985).

⁶² A discussion of results for β -brass is given by J. Als Neilsen, *Phase Transitions Crit. Phenom.* **5A**, 87 (1976).

⁶³ J. Kulik and D. de Fontaine, *Mater. Res. Soc. Symp. Proc.* **21**, 225 (1984).

⁶⁴ D. de Fontaine and J. Kulik, *Acta Metall.* **33**, 145 (1985).

⁶⁵ A. Loiseau, G. van Tendeloo, R. Portier, and F. Ducastelle, *J. Phys.* **46**, 595 (1985).

⁶⁶ J. Kulik, S. Takeda and D. de Fontaine, *Acta Metall.* **35**, 1137 (1987).

⁶⁷ R. Portier, D. Gratias, M. Guymont, and W. M. Stobbs, *Acta Crystallogr.* **A36**, 190 (1980).

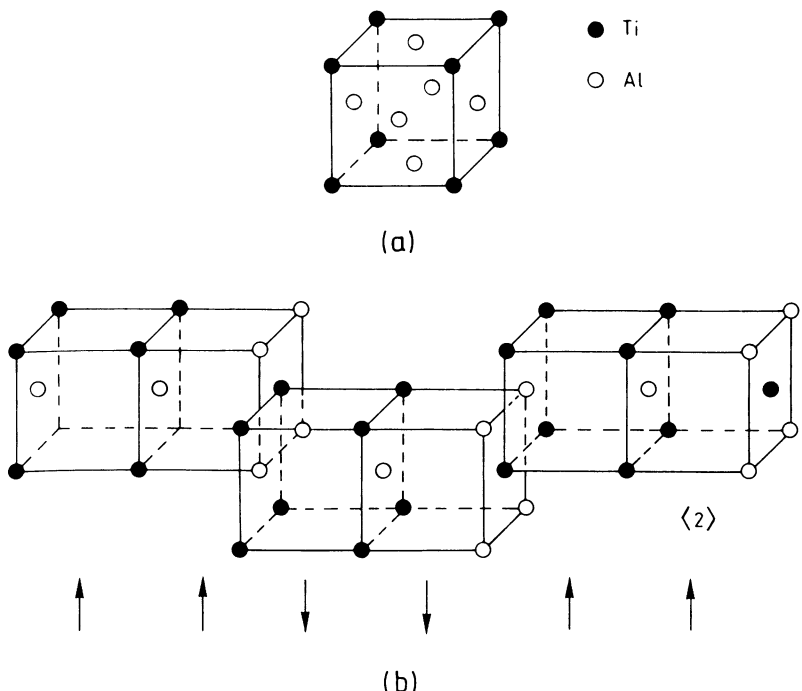


FIG. 11. Atomic structure of a binary alloy: (a) the $L1_2$ structure; (b) the $\langle 2 \rangle$ phase.

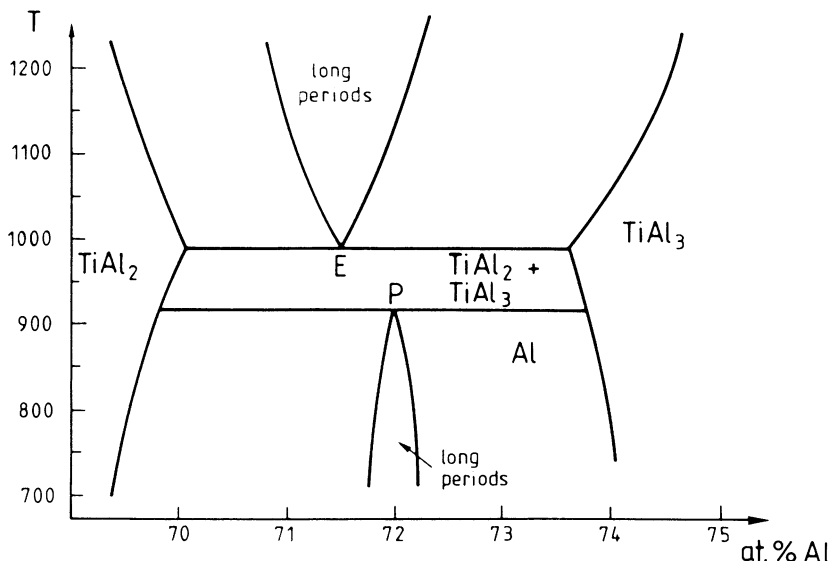
$CuAu$,⁶⁸ and Au_4Zn .⁶⁹ However, other examples, such as $TiAl_3$, are well documented.⁷⁰ These compounds have a disordered face-centered cubic structure at high temperatures. As the temperature is lowered they lock in to the $L1_2$ structure, where, taking $TiAl_3$ as an example, planes of Al alternate with mixed planes of Ti and Al along the $[001]$ direction. Within the mixed planes the two atomic species are ordered with each Al being surrounded by four Ti as nearest neighbors and vice versa. This structure is illustrated in Fig. 11a.

Modulation is introduced into the crystal structure by antiphase boundaries, as shown in Fig. 11b. Conservative antiphase boundaries, domain walls in the ANNNI model, correspond to a displacement of the Ti sublattice through $[\frac{1}{2}, \frac{1}{2}, 0]$. Hence each face-centered cube has two positions which we label \uparrow and \downarrow . Long period phases can then be described using notation analogous to the ANNNI model.⁶ For example, the phase in Fig. 11b is $\langle 2 \rangle$.

⁶⁸ M. Guymont and D. Gratias, *Acta Crystallogr. A* **35**, 181 (1979).

⁶⁹ G. van Tendeloo and S. Amelinckx, *Phys. Status Solidi A* **43**, 553 (1977).

⁷⁰ D. Broddin, G. van Tendeloo, J. van Landuyt, S. Amelinckx, R. Portier, M. Guymont, and A. Loiseau, *Philos. Mag. A* **54**, 395 (1986).

FIG. 12. Phase diagram of TiAl₃.⁶⁵

It is also possible to introduce nonconservative antiphase boundaries which change the stoichiometry of the alloy. These correspond to a displacement of $[\frac{1}{2}, 0, \frac{1}{2}]$ or $[0, \frac{1}{2}, \frac{1}{2}]$ and introduce mixed planes which are either nearest neighbors or separated by three times the interplanar spacing. These structures will be mentioned only briefly in the following.

Two beautiful sets of experiments illustrating the behavior of binary alloys have been performed on TiAl₃⁶⁵ and Cu₃Pd.⁷⁰ We shall describe the results of these experiments and discuss their interpretation in terms of the ANNNI model. The section closes with a brief mention of the behavior of other binary alloys. Reference is also given to other theoretical approaches^{71,72} which have been used to explain modulated ordering in these systems.

a. TiAl₃

Loiseau *et al.*⁶⁵ used electron diffraction and high-resolution electron microscopy to study the phase diagram of TiAl₃ for 71–73 at.% Al and temperatures between 700 and 1200 K. The phase diagram of this compound is shown in Fig. 12. Four phases are stable. Near stoichiometry, the TiAl₃ structure, which corresponds to an antiphase boundary every structural unit or $\langle 1 \rangle$, provides the stable phase. For less than 70 at.% Al two TiAl₂ structures

⁶¹ H. Sato and R. S. Toth, *Phys. Rev.* **127**, 469 (1962).

⁶² B. L. Gyorffy and G. M. Stocks, *Phys. Rev. Lett.* **50**, 374 (1983).

which contain nonconservative antiphase boundaries appear. Between these limits there are two regions of the phase diagram where different long period structures are stable, separated by a temperature range of about 100 K within which only the TiAl_3 and TiAl_2 structures are observed.

In the low-temperature stability field of the long period phases, below 900 K, only three phases were observed, $\langle 12 \rangle$, $\langle 112 \rangle$, and $\langle (12)^2 122 \rangle$. The former dominate the phase diagram. In the high-temperature range, however, a large number of different structures were found to be stable.⁶⁵

These structures are listed in Fig. 13, which shows the temperature at which each phase was observed. The experiments suggest that the structures are each

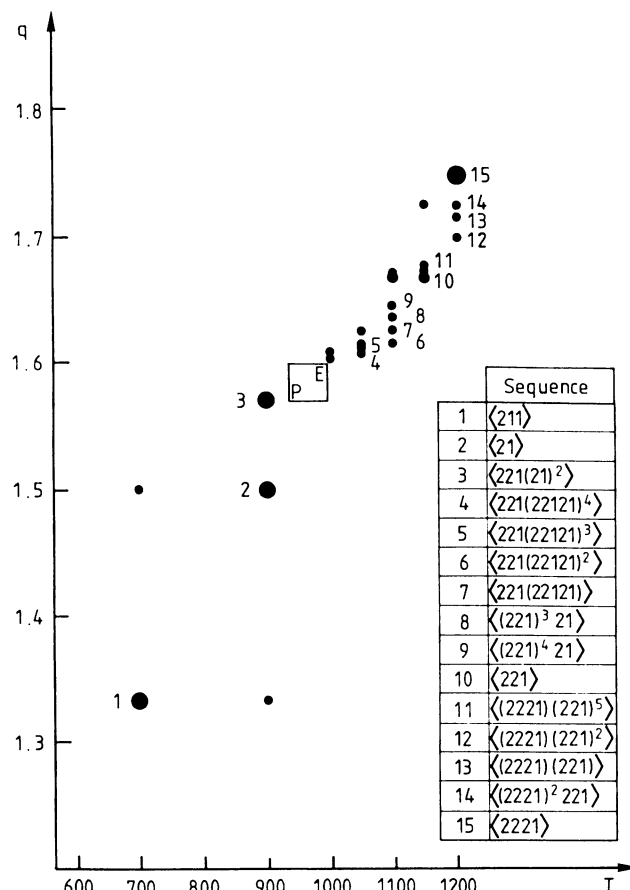


FIG. 13. Wave vector as a function of annealing temperature for the long period phases observed in TiAl_3 by Loiseau *et al.*⁶⁵

stable over a small temperature range, with the shortest period structures having the largest range of stability: about 50 K for $\langle 122 \rangle$ and $\langle (122)^2 12 \rangle$. At each annealing temperature different long period structures were found in separate areas of the sample, which may be due to variation in concentration across the sample or experimental limitations on the speed of quench, annealing time, or temperature control, producing metastability effects.

Certainly these results are very reminiscent of the behavior of the ANNNI model with antiferromagnetic first-neighbor interactions. The ordering of the long period phases observed in TiAl₃ is identical to that in the ANNNI model and in both cases the short period phases occupy the largest portion of the phase diagram. Presumably improving the resolution of the experiment would reveal the missing ANNNI phases. At lower temperatures a few commensurate phases dominate, whereas for higher temperatures a larger number of phases appear in the phase diagram, as in the case of the ANNNI model. Whether all phases have a range of stability or not, that is, whether the Devil's staircase is complete or harmless, remains an open question.

To study the compound further, Loiseau *et al.*⁶⁵ used high-resolution electron microscopy, which provides a very powerful tool in the investigation of binary alloys. It enables study of the atomic positions and, in particular, a more detailed investigation of the nature of the antiphase boundaries. With modern instruments a spatial resolution of 0.2 nm can be achieved. In general, images are taken along a cubic axis oriented perpendicular to the axial direction. Along this direction only atoms of the same species overlap, and it is easier to see any shift of the antiphase boundary throughout the thickness of the crystal (typically 10 nm). The interpretation of the electron microscope image is not straightforward, and the contrast depends strongly on the film thickness and the properties of the lens. Computer simulation of the images is necessary for a correct interpretation. However, with care, photographs can be produced where a particular atomic species corresponds to the obvious white dots on the image. An example of such a photograph where the bright dots correspond to the Ti atoms in the structure $\langle 12^3 \rangle$ is shown in Fig. 14.

One of the features emphasized by Loiseau *et al.*⁶⁵ is the appearance of jogs along certain antiphase boundaries which cause a local change in the band structure. In the $\langle 12^3 \rangle$ structure, for example, the jogs locally alter the ordering from $12^3 12^3$ to $12^2 12^4$. Similar defects can occur through movement of the boundary on every seventh plane. Hence these planes, which are indicated by arrows in Fig. 14, are diffuse in the electron microscope image. The diffuseness increases with increasing annealing temperature. These jogs can be identified with spin flips in the ANNNI model and suggest strongly that entropic effects are important in stabilizing the modulated structures. Note that the diffuse boundaries neighbor one-bands, where spin flips are more favorable because they change the spacing of one-bands rather than creating a (13) configuration.

the same sequence itself. This seems to correspond to the mechanism of grain boundary gliding but at sufficiently high temperatures it will also be possible to move the boundaries by shear without changing the orientation.

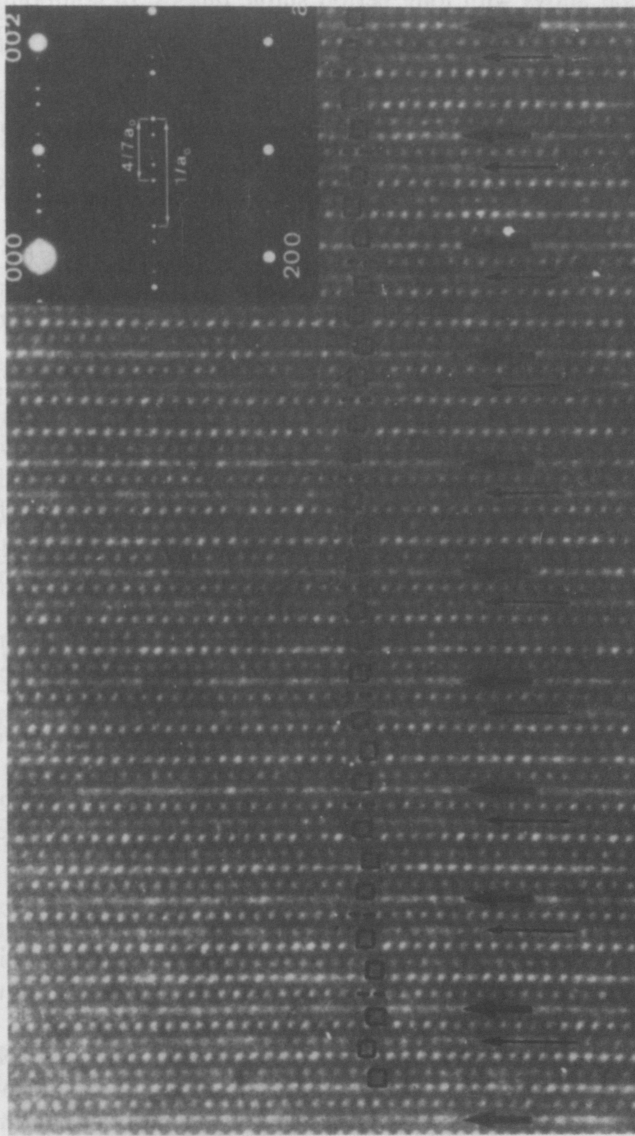


Fig. 14. High-resolution electron micrograph of the $\langle 12^3 \rangle$ structure in TiAl_3 . The arrows indicate jogged anti-phase boundaries.⁶⁵

b. Cu₃Pd

Two different types of conservative antiphase boundary have been observed in binary metal alloys with long period stable phases. In compounds such as TiAl₃ described above, the antiphase boundaries are predominantly straight,⁶⁵ whereas in alloys like CuAu they are much more diffuse and not obviously related to a (001) plane.⁶⁸ de Fontaine *et al.*⁷³ have suggested that the ability of the boundaries to wander depends on the magnitude of the in-plane coupling J_0 . Hence, well-defined antiphase boundaries would signal a compound corresponding to the low-temperature region of the ANNNI phase diagram and lockin to a series of modulated structures would be expected. Diffuse boundaries, however, would suggest higher temperatures (or equivalently smaller J_0), and the prediction that the wave vector would vary continuously, or perhaps quasicontinuously, with the external parameters and the concentration of the atomic species.

In an attempt to investigate these ideas further, Broddin *et al.*⁷⁰ have performed experiments on Cu₃Pd in the regime 17–30 at. % Pd, where one- and two-dimensional modulated structures are observed with a wave vector which varies with composition and temperature. Again electron diffraction and high-resolution electron microscopy were the techniques used. The phase space can be divided into three regions: where the L1₂ or $\langle \infty \rangle$ structure is stable, where one-dimensional long period structures are observed, and where two-dimensional long period structures are stable.

The experimental results indicate that within the one-dimensional long period regime Cu₃Pd undergoes a crossover between two distinct behaviors. For low concentrations of Pd (18–21 at. %) the commensurate phase, $\langle \infty \rangle$, is stable at low temperatures. As the temperature is raised the wave vector becomes incommensurate and decreases continuously with increasing temperature. The antiphase boundaries are very diffuse and not obviously bound to (001) planes. These results suggest that the alloy is above the depinning temperature of the domain walls.

At the other end of the concentration range considered (30 at. % Pd), however, the system locks in to short period commensurate phases. The wave vector is independent of temperature and varies discontinuously with concentration. For these concentrations the antiphase boundaries are sharp. This is typical low-temperature ANNNI behavior.

For intermediate Pd concentrations the wave vector again locks in to commensurate phases. The period of ordering is strongly dependent on the concentration and shows a slight decrease with increasing temperature. Some of the antiphase boundaries are diffuse—which ones depends strongly on the

⁷³ D. de Fontaine, A. Finel, S. Takeda, and J. Kulik, *Noble Metals Symp.* (1985).

stacking sequence itself. This seems to correspond to intermediate temperatures below depinning but at sufficiently high temperatures to allow substantial fluctuation in the softer domain walls.

Comparison of the electron microscope images with computer simulations shows that the diffuseness of the boundaries results from compositional disorder in the neighboring atomic planes. In contrast to the situation in $TiAl_3$, the diffuseness appears to be independent of the annealing temperature.

Broddin *et al.*⁷⁰ interpret their results in terms of the ANNNI model by assuming that an increase in concentration corresponds to an increase in the value of κ . Indeed it was shown by Sato and Toth⁷¹ and by Gyorffy and Stocks⁷² that the composition has a strong effect on the atomic interactions. The behavior at low concentrations then corresponds to a vertical line at a value of $\kappa < \frac{1}{2}$. The low-temperature phase is the commensurate phase $\langle \infty \rangle$, and at higher temperatures there is a transition to a region of at least quasi-incommensurate behavior. As the temperature is increased, the period would be expected to decrease with temperature, as observed experimentally.

For higher concentrations, however, the stable phases correspond to larger values of κ . Presumably the effective temperature is also lower so that less softening of the domain walls is observed in the region where modulated phases are stable.

Between the one-dimensional long period structures and the disordered face-centered cubic phase, two-dimensional modulated phases are thought to be stable over a small range of concentration. For the structure observed by Broddin *et al.*⁷⁰ the antiphase boundaries were conservative in one direction and nonconservative in the other. The corresponding periods were 4.3 ± 0.1 and 6.3 ± 0.1 , respectively. Other domain sizes have been observed by other authors.⁷⁴ Since the two-dimensional modulated structures only exist over a small range it was not possible to study the evolution of their domain sizes as a function of temperature or composition. One might guess that these phases are a result of competing interactions in two directions. Little is known about a corresponding Ising model (but see Refs. 49 and 50), and any work on the nature of the phase diagram of such a model would be of great interest.

c. Other Compounds and Theories

The appearance of long-wavelength phases in binary alloys is by no means limited to the compounds described above. Another notable example is Ag_3Mg , where $\langle 12^j \rangle$ with $j = 2, 3, \dots, 7, 8, 12$ have been observed together with the mixed phases $\langle 12^2 12^3 \rangle$ and $\langle 12^3 12^4 \rangle$.^{66,67} A recent experimental

⁷⁴ O. Terasaki and D. Watanabe, *Jpn. J. Appl. Phys.* **20**, L381 (1981).

study of this compound⁶⁶ attempted to discern the concentration and temperature dependence of the period. However, this proved to be very difficult because of sluggish kinetics. $\langle 2 \rangle$, $\langle 2^3 3 \rangle$, and $\langle 3 \rangle$ have been identified in Au_4Zn .⁶⁹ In CuAu the antiphase domain boundaries are much more diffuse and wavy and the modulation is probably incommensurate with the lattice.⁶⁸

The existence of incommensurate phases in binary alloys has, until recently, been explained using ideas proposed by Sato and Toth.⁷¹ They argued that incommensurate order could be stabilized by energy gained from the interaction between the Fermi surface and the new Brillouin zone boundaries resulting from the periodic modulation. Gyorffy and Stocks⁷² later performed band theory calculations supporting this picture for Cu_3Pd . These ideas naturally explain the concentration dependence of the period of the modulated order but do not account for temperature effects nor predict locking to commensurate phases.^{75,76} The ANNNI picture allows the latter to be investigated but does not relate J_1 and J_2 to microscopic interactions. An amalgam of the two approaches in which band theory calculations are used to provide values for J_1 and J_2 and assess the effects of further-neighbor interactions would be very interesting.

7. POLYTYPISM

We now turn to a second class of materials exhibiting modulated structures, the polytypes.^{77,78} The experimental situation here is far less clear, but, although metastability effects are very important, there is growing evidence to suggest that the modulated structures in these compounds can exist as stable phases which are well described by ANNNI-like Hamiltonians.⁷⁹⁻⁸⁴

It is helpful in many cases to consider a compound to be constructed from one or more individual building blocks or structural units.⁸⁵ If the units can be stacked in different ways to form several stable or metastable phases, the

⁷⁵ K. Fujiwara, *J. Phys. Soc. Jpn.* **12**, 7 (1957).

⁷⁶ D. de Fontaine, *J. Phys. A: Math. Gen.* **17**, L713 (1984).

⁷⁷ A. R. Verma and P. Krishna, "Polymorphism and Polytypism in Crystals." Wiley, New York (1966).

⁷⁸ P. Krishna (ed.), *J. Cryst. Growth Charact.* **7** (Spec. Issue) (1984).

⁷⁹ S. Ramasesha, *Pramana* **23**, 745 (1984).

⁸⁰ J. M. Yeomans and G. D. Price, *Bull. Mineral.* **109**, 3 (1986).

⁸¹ G. D. Price and J. M. Yeomans, *Acta Crystallogr.* **B40**, 448 (1984).

⁸² J. Smith, J. M. Yeomans, and V. Heine, *NATO ASI Ser., Ser. E* **83**, 95 (1984).

⁸³ R. M. Hazen and L. W. Finger, in "Structure and Bonding in Crystals II" (M. O'Keeffe and A. Navrotsky, eds.), p. 109. Academic Press, New York, 1981.

⁸⁴ G. D. Price, *Phys. Chem. Miner.* **10**, 77 (1983).

⁸⁵ J. B. Thompson, in "Structure and Bonding in Crystals II" (M. O'Keeffe and A. Navrotsky, eds.), p. 167. Academic Press, New York, 1981.

resulting compounds are called polytypes.^{77,78} Polytypism is surprisingly common in nature. Perhaps the best known examples are the classical polytypes⁸⁶ such as silicon carbide and cadmium iodide, where the *A*, *B*, *C* stacking sequence of the close-packed layers can vary. Over one hundred different structures have been observed in silicon carbide with repeat periods up to ~ 100 layers. Polytypic modifications are also found in the spinelloids, perovskites, micas, pyroxenes, chlorites, and many other mineral phases.

The reasons for the appearance of numerous, but often closely related, polytypic phases and the extent to which the various phases are stable or metastable has been very controversial. Two main classes of theories have been mooted. Growth theories^{86,87} assume that the modulated structure of the polytype results from growth around a screw dislocation with a period that reflects the step height of the dislocation. Equilibrium theories,^{80,88} on the other hand, assume that the polytypic modifications can exist as stable thermodynamic phases, while admitting that equilibration is a problem in real systems.

It has recently been pointed out that the ANNNI and similar models reproduce many of the properties of the polytypic phases.⁷⁹⁻⁸⁴ Indeed, invoking short-range competing interactions gives a rather convincing explanation of their existence. We discuss two cases in detail: first, the spinelloids and second, the classical polytypes such as silicon carbide and cadmium iodide. Other theories of polytypism are briefly reviewed and the extension of the theory to treat polysomatic compounds is discussed.

a. The Spinelloids

The spineloid structural family⁸⁹ is based upon an approximately close-packed oxygen framework and has an ideal stoichiometry of AB_2O_4 , where *A* and *B* represent cations such as nickel and aluminum. Two-thirds of the cations occupy octahedrally coordinated sites within the O framework, while the remaining one-third are tetrahedrally coordinated. The cations define a basic structural unit within the oxygen framework, as shown in Fig. 15. All spineloid structures are constructed from this unit, (\uparrow), and its inverse, (\downarrow), and hence the structures can be mapped onto an array of structural variables which are Ising spins.

In almost all spineloids the ordering within two-dimensional layers corresponds to an Ising ground state which is ferromagnetic in one direction and antiferromagnetic in the perpendicular direction. Perpendicular to the

⁸⁶ D. Pandey and P. Krishna, *J. Cryst. Growth Charact.* **7**, 213 (1984).

⁸⁷ F. C. Frank, *Philos. Mag.* **42**, 1014 (1951).

⁸⁸ H. Jagodzinski, *Neues. Jahrb. Mineral., Monatsh.* **3**, 49 (1954).

⁸⁹ H. Horiuchi, K. Horioka, and N. Morimoto, *J. Mineral Soc. Jpn.* **2**, 253 (1980).

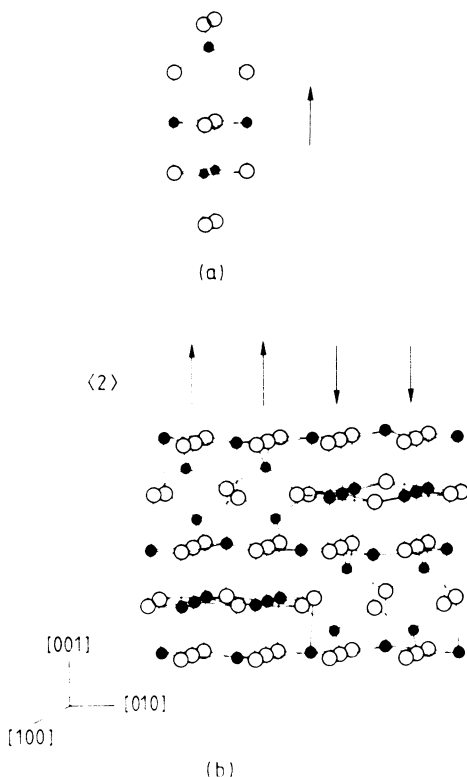


FIG. 15. Atomic structure of the spinelloids: (a) a structural unit; (b) the $\langle 2 \rangle$ phase.

invariant layers, however, six different stacking sequences are observed in nature. These, using the ANNNI notation to describe them, are the spinel phase, $\langle 1 \rangle$, the β phase, $\langle 2 \rangle$, the manganostibite structure, $\langle 3 \rangle$, and three structures found only in the Ni_2SiO_4 - NiAl_2O_4 system, $\langle 12 \rangle$, $\langle 12^2 \rangle$, and $\langle 13 \rangle$.

To model these systems we assume that the important interactions between the atoms in any pair of structural units can be represented by an interaction between the corresponding structural variables.⁷⁹⁻⁸² The correct in-plane ordering will result if the Ising spins interact through nearest-neighbor interactions which are ferromagnetic in one direction and antiferromagnetic in the other. However, the appearance of longer period structures along the axial direction suggests that the further-neighbor interactions are of the same magnitude as the nearest-neighbor terms. Hence one is led to represent the system using an ANNNI model.

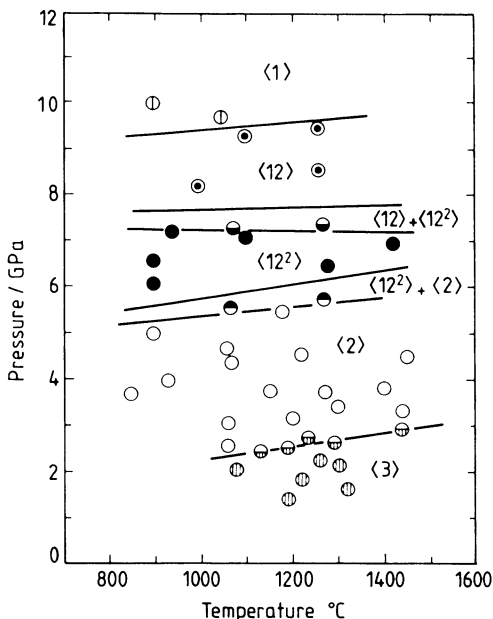


FIG. 16. Phase diagram of the system $\text{NiAlO}_4 \cdot \text{Ni}_2\text{SiO}_4$.⁹⁰

The assumption then is that, as external parameters such as temperature and pressure are varied, the atomic positions and hence interactions change slightly. This can result in a change in the ratio of the interaction parameters, J_i , which, together with the variation in the temperature, moves the system through the phase space of the ANNNI model.

Perhaps the most convincing evidence for these ideas results from the work of Akaogi *et al.*,⁹⁰ who studied the phase relationships for the system $\text{NiAl}_2\text{O}_4 - \text{Ni}_2\text{SiO}_4$ in the pressure range 1.5–13.0 GPa for temperatures between 800 and 1450°C. They found that, as the pressure was increased, the sequence of structures <3>, <2>, <12²>, <12>, and <1> became stable, as shown in Fig. 16. This bears a striking resemblance to the stable phase sequence in the ANNNI model phase diagram. The missing long period phases do not pose a problem as they would not be expected to lie within the resolution of the experiment.

The interaction parameters in the model Hamiltonian have been introduced on a purely phenomenological level to represent the energy difference between structural units which are aligned parallel or antiparallel. However, they are in

⁹⁰ M. Akaogi, S. Akimoto, K. Horioka, K. Takahashi, and H. Horiuchi, *J. Solid State Chem.* **44**, 257 (1982).

theory related to the microscopic interactions in the system which will depend on temperature, pressure, and chemical composition.

In an attempt to obtain quantitative values for the parameters, Price *et al.*⁹¹ used lattice simulation techniques to calculate the interaction energies of the structural units in magnesium silicate spinelloids. Using two different model potentials and assuming pair interactions up to fourth-neighbor spins, they found

$$J_2/J_1 = 0.45, \quad J_3/J_1 = -0.36, \quad J_4/J_1 = 0.23, \quad J_1 < 0 \quad (7.1)$$

$$J_2/J_1 = 0.56, \quad J_3/J_1 = -0.00, \quad J_4/J_1 = 0.01, \quad J_1 < 0 \quad (7.2)$$

These sets of results are both consistent with interactions lying within the multiphase region of the ANNNI model and support its use to interpret polytypism. Although further-neighbor interactions are inevitably present, they do not qualitatively change the nature of the phase sequences, as shown in Section 4.b.

A problem which it would be interesting to resolve is the apparent stability of the $\langle 13 \rangle$ spineloid phase, which does not fit into the ANNNI framework. The $\langle 13 \rangle$ phase, which has also been observed in other polytypic compounds, has not appeared in any of the models studied so far except the ANNNI model in a magnetic field.⁴⁰

A similar mineral is wollastonite, where the phases $\langle 2 \rangle$, $\langle 3 \rangle$, $\langle 4 \rangle$, $\langle 5 \rangle$, and $\langle \infty \rangle$ have been observed. The different symmetries of this compound suggest that it is best modeled by competing interactions between second- and fourth-neighbor layers.⁹²

b. Classical Polytypes

We now return to the so-called classical polytypes.⁸⁶ These have MX or MX_2 stoichiometry and are characterized by SiC and CdI₂, respectively. Their structures consist of planes of M atoms, each of which is tetrahedrally coordinated with X atoms which are stacked in a close-packed array. The MX structures can be considered as a pair of interpenetrating close-packed sublattices with alternating layers of M and X atoms. Therefore, the entire crystal structure can be uniquely specified by the stacking sequence of the X layers. In the MX_2 structure, however, the M atoms occupy only alternate planes of tetrahedral sites between the layers of X atoms so that the structure is a stack of $X-M-X$ "sandwiches." Using the convention that the first layer in a stacking sequence is chosen to lie immediately to the left of an M layer, the polytype can again be defined by the stacking sequence of the X layers.

⁹¹ G. D. Price, S. C. Parker, and J. M. Yeomans, *Acta Crystallogr.* **B41**, 231 (1985).

⁹² R. J. Angel, G. D. Price, and J. M. Yeomans, *Acta Crystallogr.* **B41**, 310 (1985).

It is conventional to describe the stacking sequence of a given polytypic compound using a notation introduced by Zdhanov and Minervina,⁹³ which turns out to closely resemble that which we have used throughout to describe the long period phases in the ANNNI model. Zdhanov notation emphasises the fact that a close-packed stack of layers can be thought of as a two-state system because any given layer, say one in position *A*, can only be followed by layers in two possible positions, *B* and *C*. This is done by assigning \uparrow to represent the stackings *A*-*B*, *B*-*C*, and *C*-*A* and \downarrow to represent anticyclic ordering, *B*-*A*, *C*-*B*, and *A*-*C*. For example, a given stacking sequence is

$$\begin{array}{ccccccccccccccccc} A & B & C & A & C & B & A & B & C & A & C & B & A & B & C & A & C & B \\ \uparrow & \uparrow & \uparrow & \downarrow & \downarrow & \downarrow & \uparrow & \uparrow & \uparrow & \downarrow & \downarrow & \downarrow & \uparrow & \uparrow & \uparrow & \downarrow & \downarrow & \downarrow \end{array} \quad (7.3)$$

which as usual we denote $\langle 3 \rangle$.

Consider first SiC. A very large number of polytypes have been observed,^{86,94} although in many cases the evidence for their existence as true thermodynamically stable phases is very slim. However, the stable and metastable phases which are documented have the following striking properties:

- (1) The short period structures $\langle 3 \rangle$, $\langle 2 \rangle$, $\langle 23 \rangle$, $\langle \infty \rangle$, and $\langle 1 \rangle$ are by far the most commonly observed.
- (2) Transformations have been observed between the short period polytypes.⁹⁴ However, these often rely on the addition of impurities or the application of pressure and are hence far from being reversible.
- (3) Trivalent impurities, such as boron and aluminum, tend to favor two-bands, whereas pentavalent impurities favor cubic stacking ($\langle \infty \rangle$).
- (4) In the longer period structures three-bands predominate. Two-bands are also rather common, and four- and longer bands are seen occasionally. One-bands are only observed in the phase $\langle 1 \rangle$.
- (5) Long period structures can usually be formed from the simple phases through the usual structure combination rules. Indeed, Pandey and Krishna⁸⁶ have suggested (for different purposes) that the observed phases fall rather neatly into ANNNI-like sequences.
- (6) Disordered structures, with no well-defined wave vector, are also common and may often have been documented as long period phases.

These features are well explained by modeling silicon carbide with an ANNNI model with the Zdhanov variables taking the role of the Ising spins.⁷⁹⁻⁸² A large value of J_0 then ensures little disorder within the close-packed layers, whereas competing interactions along the axial direction allows

⁹³ G. S. Zdhanov and Z. Minervina, *Zh. Fiz.* **9**, 151 (1945).

⁹⁴ N. W. Jepps and T. F. Page, *J. Cryst. Growth Charact.* **7**, 259 (1984).

the formation of a large number of polytypes. The best qualitative agreement is with the axial Ising model with third-neighbor interactions in the vicinity of the $\langle 2 \rangle : \langle 3 \rangle$ and $\langle 3 \rangle : \langle \infty \rangle$ multiphase lines.³³ Here $\langle 2 \rangle$, $\langle 3 \rangle$, and $\langle \infty \rangle$ appear as ground-state phases and dominate the phase diagram, and $\langle 23 \rangle$ appears as an important finite-temperature phase near the $\langle 2 \rangle : \langle 3 \rangle$ boundary. The fifth common polytypic phase $\langle 1 \rangle$ would be stabilized by a change in the sign of J_1 .

All the transformations between the short period phases⁹⁴ correspond to obvious routes between neighboring phases in the ANNNI phase diagram. As was argued in Section 4.c, annealed impurities are not expected to destabilize the long period structures.³⁴ The observed effect of impurities can be explained by assuming that the addition of acceptors tends to increase κ , whereas donors tend to decrease it.

Moreover, the long period phases observed in silicon carbide bear a striking resemblance to the phase sequences which are stable in this region of the phase diagram.⁸⁶ Both the predominance of 2- and 3-bands and the arrangement of the bands within a given phase are suggestive of the same mechanism at work.

It is of course the case that metastability effects are extremely prevalent in SiC. A batch of crystals grown under nominally the same conditions will contain many different polytypes, even within the same single crystal. The ANNNI picture is also able to explain why it is so difficult to obtain the true thermodynamically stable phase. In the vicinity of the multiphase lines the free energy of the long-wavelength phases which are degenerate on the line itself differ only by very small entropic contributions (typically less than one part in 10^4). Moreover, transitions between the different energy states require a substantial rearrangement of atoms, and hence the energy barrier inhibiting the transitions is very large. Thus, once a compound has formed in a metastable state due, for example, to the effect of growth conditions, it is likely to stay there. The disordered structures often observed are also expected to be metastable.

One should point out that a major defect of the ANNNI model as a theory of silicon carbide is that it does not accurately mirror the elementary excitations of the compound: an ANNNI spin flip would correspond to flipping a single line of atoms from the flip itself to the edge of the crystal, which is clearly unphysical.

Note, however, that in the Villain and Gordon formulation of the mean-field theory of the ANNNI model,¹⁵ described in Section 3.b, individual spin flips are replaced by the average deviation of the spins within a layer from their zero temperature value. Thus, it may be the case that small deviations throughout a plane of atoms caused by, for example, phonons, can stabilize the long period phases.

Cadmium iodide is usually quoted as an example of the MX_2 classical polytypes. For this compound over 50 phases have been observed. One- and two-bands predominate in the long period structures, which suggests that CdI₂ is best modeled by the ANNNI model with negative J_1 .^{81,82} It is interesting to note, however, that several of the long period phases observed in this compound (for example, $\langle 1^{n_1}, 2^{n_2} \rangle$, n_1 , n_2 positive integers) cannot be constructed using the structure combination branching rules.

A third classical polytype with interesting behavior is zinc sulfide.⁹⁵ For this compound polytypism in mineralogical samples differs from that observed in laboratory grown crystals. In the latter almost any band length can occur and the screw dislocation mechanism is well documented. In mineralogical samples, however, which have had time to come to equilibrium, the observed phases are $\langle \infty \rangle$, $\langle 5 \rangle$, $\langle 4 \rangle$, $\langle 3 \rangle$, $\langle 23 \rangle$, $\langle 2 \rangle$, $\langle 12 \rangle$, and $\langle 2 \rangle$, which correspond closely to the ANNNI phases, and $\langle 13 \rangle$ and $\langle 1123 \rangle$, which do not. A study of many polytypic crystals obtained from a mine bore indicated that the structure was a function of depth.⁹⁶

For comparison we briefly summarize other theories of polytypism in the classical polytypes. Jagodzinski⁸⁸ was the first to propose an equilibrium theory of polytypism. He argued that the vibrational entropy would provide a term in the free energy which would stabilize the long period structures. However, this theory is unable to correctly predict the fault distribution in the long period polytypes. More recently Hazen and Finger⁸³ and Price⁸⁴ explained the existence of short period polytypes in terms of the ground state of the axial Ising model with third-neighbor interactions.

Growth theories of polytypism, on the other hand, regard the long period polytypes as nonequilibrium structures which result from growth around screw dislocations.^{86,87} The period of a given polytype is then determined by the step height of the growth spiral. The problem with these theories is that they cannot predict which of the long period phases actually occur in nature. Moreover, very large, and hence energetically unfavorable, steps would often be needed.

A recent, interesting modification of this theory has considered the influence of low-energy stacking faults present near the surface of the basic matrix, $\langle 3 \rangle$, $\langle 2 \rangle$, or $\langle \infty \rangle$, on the spiral growth.^{86,97} Consideration of such a faulted matrix model enables the prediction of sequences of structures very close to those observed in silicon carbide. However, there is as yet no convincing way of deciding which of the possible series one should expect to occur in nature.

⁹⁵ I. T. Steinberger, *J. Cryst. Growth Charact.* **7**, 7 (1984).

⁹⁶ S. Hussuhl and G. Muller Beitr. *Z. Miner. Petrogr.* **9**, 28 (1963).

⁹⁷ D. Pandey and P. Krishna, *Curr. Top. Mater. Sci.* **9**, 415 (1981).

There are, however, many interesting links between these ideas and the ANNNI picture. For example, Pandey and Krishna⁸⁶ use a model in many ways similar to the ANNNI model at zero temperature in determining which of the stacking fault configurations are expected to occur most frequently.

c. Polysomaticism

A similar approach has been applied to explaining the occurrence of polysomatic series.⁹⁸ These materials correspond to families of structures which can be obtained by stacking in varying proportions two or more chemically distinct units, *A* and *B*, say.⁹⁹ An example is the biopyriboles, where *A* represents mica and *B* pyroxene layers.¹⁰⁰ The observed phases are then $\langle A \rangle$, $\langle AB \rangle$, $\langle AABAB \rangle$, $\langle A.AB \rangle$, and $\langle B \rangle$. Replacing *A* and *B* by \uparrow and \downarrow , respectively, one again obtains ANNNI-like phases. A chemical potential term is needed to control the relative abundance of the two species, and hence the appropriate spin model is the ANNNI model in a magnetic field.

One hopes that using ANNNI-like models to describe ordering in polytypes will encourage the view that long period modulated structures can exist as stable thermodynamic phases in compounds where the atomic interactions are predominantly short ranged. Hence it is hoped that experimental effort will be directed toward the difficult task of establishing phase diagrams for polytypic compounds.

The model systems are useful in predicting which phase sequences will be stable and the expected distribution of bands within a given phase. Moreover, predictions can be made which hopefully can be verified experimentally, about defect distributions and the relative probability of occurrence of different types of dislocation. It would be of great interest to pursue further calculations which relate the phenomenological energies J_i , $i = 0, 1, 2, \dots$, to the atomic interactions in the polytypic compounds.^{91,101}

8. MAGNETIC SYSTEMS

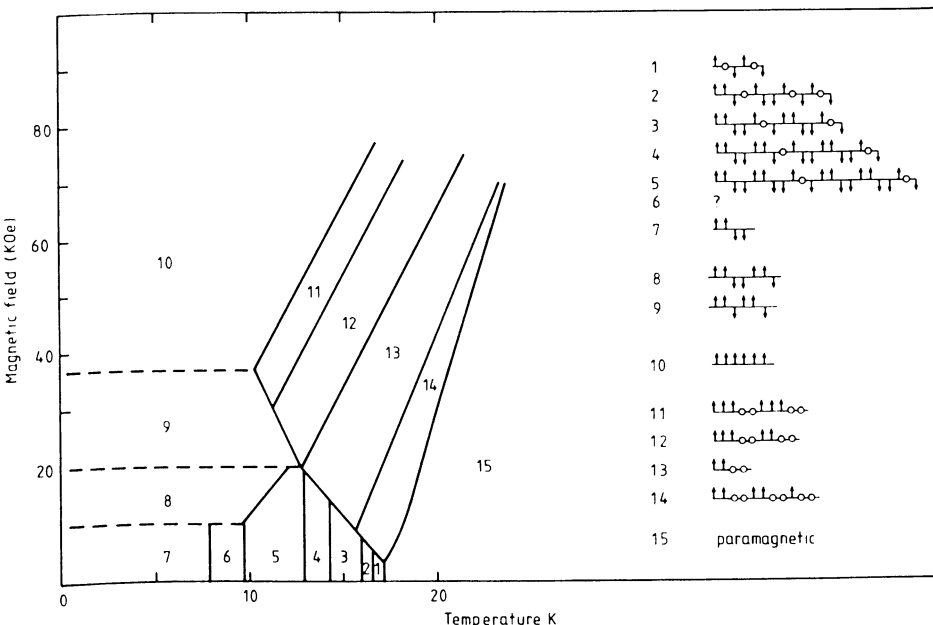
The best candidates for ANNNI systems where the Ising variables correspond to magnetic spins are found among the cerium monopnictides. In cerium antimonide strong uniaxial spin anisotropy constrains the spins to point along the [100] direction. Within the (100) planes the ordering is ferromagnetic: most planes lie in a state with saturated magnetization along or

⁹⁸ G. D. Price and J. M. Yeomans, *Min. Mag.* **50**, 149 (1986).

⁹⁹ J. B. Thompson, *Am. Mineral.* **63**, 239 (1978).

¹⁰⁰ D. R. Veblen and P. R. Buseck, *Am. Mineral.* **64**, 687 (1979).

¹⁰¹ C. Cheng, R. J. Needs, V. Heine, and N. Churcher, *Europhys. Lett.* **3**, 475 (1987).

FIG. 17. Phase diagram of cerium antimonide.¹⁰⁷

antiparallel to the axial direction. However, at first sight, rather surprisingly, planes with zero magnetization also appear for temperatures $\gtrsim T_N/2$, where the Néel temperature, $T_N = 17$ K. The ferromagnetic planes form modulated structures with a wave vector along [100], which locks into different values as a function of temperature and magnetic field.

Cerium antimonide has been extensively studied by neutron scattering¹⁰²⁻¹⁰⁶ and specific heat measurements.¹⁰⁷ The experiments give consistent results, although there are small differences between samples. The resulting phase diagram, which comprises 14 commensurate phases, is shown in Fig. 17.¹⁰⁷ We give the layer configurations rather than the Zdhanov notation for each phase to emphasize the appearance of the layers with zero magnetization. It is apparent from Fig. 17 that the stable phases can rather

¹⁰² B. Lebech, K. Clausen, and O. Vogt, *J. Phys. C* **13**, 1725 (1980).

¹⁰³ P. Fischer, B. Lebech, G. Meier, B. D. Rainford, and O. Vogt, *J. Phys. C* **11**, 345 (1978).

¹⁰⁴ G. Meier, P. Fischer, W. Halg, B. Lebech, B. D. Rainford, and O. Vogt, *J. Phys. C* **11**, 1173 (1978).

¹⁰⁵ J. Rossat-Mignod, P. Burlet, J. Villain, H. Bartholin, T.-S. Wang, D. Florence, and O. Vogt, *Phys. Rev. B* **16**, 440 (1977).

¹⁰⁶ P. Burlet, J. Rossat-Mignod, H. Bartholin, and O. Vogt, *J. Phys.* **40**, 47 (1979).

¹⁰⁷ J. Rossat-Mignod, P. Burlet, H. Bartholin, O. Vogt, and R. Langier, *J. Phys. C* **13**, 6381 (1980).

naturally be grouped into three classes:

- (1) 1–7, which form the zero-field sequence as the temperature is lowered;
- (2) 7–10, which appear as the magnetic field is increased at low temperatures; and
- (3) 10–14, which appear at higher temperatures and fields. All the phase transitions are first order.¹⁰²

von Boehm and Bak¹⁶ were the first to point out that the behavior of cerium antimonide could be explained by invoking short-range competing interactions. In an attempt to obtain a more quantitative fit to the experimental data, Pokrovsky and Uimin^{31,36} studied the ANNNI model in a magnetic field (see Section 4.a) in the regime $J_0 \gg J_1$ with small third- and fourth-neighbor couplings. They obtained a phase diagram which topologically rather closely resembles that of cerium antimonide, and they identified the three sets of phases as belonging to the sequences

- (1) $\langle 1^2 2^{2k+2} \rangle$
- (2) $\langle 12^{2k+1} \rangle$
- (3) $\langle 12(13)^2 \rangle, \langle 13 \rangle, \langle 14 \rangle, \dots$

They pointed out that the zero magnetization layers could not be disordered but gave no explanation of their existence.

One possible explanation of the zero magnetization layers in sequence (1) is that they lie in the same position as the fluctuating domain boundaries observed in the binary alloys.⁶⁵ This immediately suggests that the sequence is $\langle 12^{k+1} \rangle$ (although $\langle 12^2 \rangle$ is replaced by $\langle 12(12^2)^2 \rangle$) with the boundary between the one- and two-bands fluctuating to give local order $\langle 12^k 12^{k+2} \rangle$ on a time scale short compared to that of the experiment. Another possibility is that higher order magnetic interactions are important in this material.^{107a}

Two other features of the phase diagram which require explanation are, first, why the transition to the paramagnetic phase does not proceed via a region of incommensurate order and, second, why the longer period, rather than the shorter period, phases appear to be stable over wider ranges of temperature.

Cerium bismuth is a similar compound where modulated magnetic phases have been observed.¹⁰⁸ The phases $\langle 1 \rangle, \langle 2 \rangle, \langle 12^5 \rangle, \langle 13 \rangle, \langle 1^3 3 \rangle$, and $\langle 1^3 313 \rangle$ are stable, and no layers of zero magnetization appear. This system has been

^{107a} B. Hälg and A. Furrer, *Phys. Rev.* **B34**, 6258 (1986).

¹⁰⁸ H. Bartholin, P. Burlet, S. Quezel, J. Rossat-Mignod, and O. Vogt, *J. Phys., Colloq.* **40**, C5 (1979).

studied by Uimin¹⁰⁹ using an axial Ising model with first-, second-, and third-neighbor interactions in a magnetic field. His results reproduce the experimental phase diagram rather well.

9. CONCLUSION

The experiments described above give convincing evidence for the applicability of the ANNNI model to natural phenomena. The model provides a mechanism through which polytypes can exist as equilibrium or highly metastable states and therefore challenges conventional growth theories and encourages experiments on the stability and kinetics of phase transformations in these compounds. It provides an explanation for commensurate modulated order in binary alloys and ferrimagnets and for the phase sequences observed and their dependence on temperature. Moreover, the formalism is sufficiently simple that the effects of defects and changes in the Hamiltonian can be assessed.

Having espoused the cause of the ANNNI model, it is important now to point out the drawbacks of this approach and areas where further research is needed. First, the interaction parameters, J_i , $i = 0, 1, \dots$, are introduced phenomenologically and their magnitude is inferred by fitting to the experimental results. Initial attempts have been made to calculate the effective interactions from first principles using band theory¹⁰¹ and atomic modeling techniques,⁹¹ and the calculations, although difficult, are well worth pursuing.

A second point that warrants emphasis is the role of long-range interactions. It was shown in Section 3,b that the ANNNI model can be mapped onto a system of domain walls with long-range oscillatory interactions.^{11,15} In the ANNNI model the interactions are a result of entropy: of local fluctuations in the wall positions at finite temperatures. However, other physical mechanisms, for example elastic interactions or, in metals, electronic terms, could play the same role.

Bruinsma and Zangwill¹¹⁰ describe one approach which invokes long-range interactions in an interesting paper which considers magnesium-based, Friauf–Laves-phase ternary alloys. These compounds lock in to an ANNNI-like sequence of phases— $\langle 1^22 \rangle$, $\langle 1^2212 \rangle$, $\langle 12 \rangle$, $\langle 1212^2 \rangle$, $\langle 12^2 \rangle$, $\langle 12^3 \rangle$, $\langle 12^4 \rangle$, $\langle 2 \rangle$, $\langle \infty \rangle$, $\langle 3 \rangle$, $\langle 2 \rangle$ —as a function of the number of valence electrons per atom.¹¹¹ Bruinsma and Zangwill¹¹⁰ calculate the free energy of a domain

¹⁰⁹ G. V. Uimin, *J. Phys., Lett.* **43**, L665 (1982).

¹¹⁰ R. Bruinsma and A. Zangwill, *Phys. Rev. Lett.* **55**, 214 (1985).

¹¹¹ Y. Komura and Y. Kitano, *Acta Crystallogr.* **B33**, 2496 (1977).

wall and nearest-neighbor interactions between walls from the pair potentials of pseudopotential theory. These interactions stabilize the polytypes $\langle 2 \rangle$, $\langle \infty \rangle$, and $\langle 12 \rangle$. The degeneracy on the boundaries between these phases is then lifted to stabilize the longer period phases by invoking elastic interactions.

This and similar calculations¹¹² emphasize that either temperature or long-range interactions can stabilize modulated phase sequences. Evidence for the former is found in fluctuations in the domain walls. These have been seen in binary alloys and ferrimagnets but not yet in polytypes like SiC or the Friauf–Laves phases. This is an important problem, and more experimental and theoretical work is needed.

We conclude by considering the transition from cubic to hexagonal close packing. Within the ANNNI formalism this corresponds to a transition, $\langle \infty \rangle \rightarrow \langle 1 \rangle$, at which J_1 changes sign. J_2 will therefore be important, and, if it is antiferromagnetic, competition can result in modulated phases. This suggests that polytypism should be rather common in the vicinity of structural phase transformations.¹¹³ There is some evidence for this in metals and in recent experiments which show the appearance of tweed—incommensurate regions—near a martensitic transformation.¹¹⁴

ACKNOWLEDGMENTS

I should like to thank my colleagues for enjoyable collaborations and discussions on the topics treated in this article. Thanks are also due to NORDITA, Copenhagen, for kind hospitality while part of the review was written.

¹¹² P. Bak and R. Bruinsma, *Phys. Rev. Lett.* **49**, 249 (1982).

¹¹³ A. Zangwill and R. Bruinsma, *Comments Condens. Matter Phys. B* **13**, 1 (1987).

¹¹⁴ L. E. Tanner, A. R. Pelton, and R. Gronsky, *J. Phys., Colloq.* **43**, C4-169 (1982).